

REC'D 26 OCT 2004

WIPO

PCT

PA 1237464

# THE UNITED STATES OF AMERICA

TO ALL TO WHOM THESE PRESENTS SHALL COME:

UNITED STATES DEPARTMENT OF COMMERCE

United States Patent and Trademark Office

October 19, 2004

THIS IS TO CERTIFY THAT ANNEXED HERETO IS A TRUE COPY FROM THE RECORDS OF THE UNITED STATES PATENT AND TRADEMARK OFFICE OF THOSE PAPERS OF THE BELOW IDENTIFIED PATENT APPLICATION THAT MET THE REQUIREMENTS TO BE GRANTED A FILING DATE UNDER 35 USC 111.

APPLICATION NUMBER: 60/484,571

FILING DATE: July 02, 2003

NZ / 04 / 141

**PRIORITY DOCUMENT**  
SUBMITTED OR TRANSMITTED IN  
COMPLIANCE WITH  
RULE 17.1(a) OR (b)

By Authority of the  
COMMISSIONER OF PATENTS AND TRADEMARKS



*Trudie Wallace*  
TRUDIE WALLACE

Certifying Officer

BEST AVAILABLE COPY

15541 U.S. PTO  
07/02/03

Attorney Docket No. 9405-3PR

PATENT

**COVER SHEET FOR FILING PROVISIONAL  
PATENT APPLICATION (37 CFR §1.51(c)(1))**

Mail Stop PROVISIONAL PATENT APPLICATION  
Commissioner for Patents  
P.O. Box 1450  
Alexandria, VA 22313-1450

Date: July 2, 2003

16015 U.S. PTO  
60/484571  
07/02/03

This is a request for filing a PROVISIONAL PATENT APPLICATION under 37 C.F.R. §1.53(c).

Docket No.	9405-3PR
Type a plus sign (+) inside this box <input type="checkbox"/>	+

INVENTOR(s)/APPLICANT(s)

Name: Adnan Anbuky  
Address: New Zealand

Name: Phillip Hunter  
Address: New Zealand

TITLE OF THE INVENTION (280 characters maximum)

**BATTERY FLOAT MANAGEMENT**

ENCLOSED APPLICATION PARTS (check all that apply)

- ☒ Specification (Number of Pages 62)
- ☐ Drawing(s) (Number of Sheets     )
- ☐ Claims (Number of Claims     )  
(A complete provisional application does not require claims 37 C.F.R. §1.51(c)).
- ☐ Application Data Sheet. See 37 CFR §1.76
- ☐ Other:

Attorney Docket No.: 9405-3PR  
Filed: Concurrently Herewith  
Page 2

CORRESPONDENCE ADDRESS



20792

PATENT TRADEMARK OFFICE

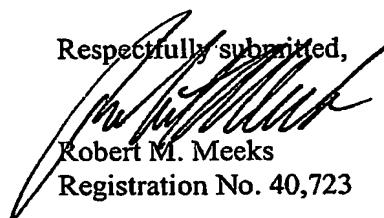
METHOD OF PAYMENT

- ☐ Applicant claims small entity status. See 37 CFR §1.27.  
☒ Check or money order is enclosed to cover the filing fee.  
☐ Payment by credit card. Form PTO-2038 is attached.  
☒ The Commissioner is hereby authorized to charge filing fees or credit any overpayment to Deposit Account No. 50-0220.

The invention was made by an agency of the United States Government or under a contract with an agency of the United States Government.

- ☒ No.  
☐ Yes, the name of the U.S. Government agency and the Government contract number are:

Respectfully submitted,

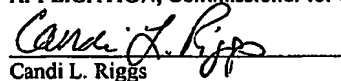


Robert M. Meeks  
Registration No. 40,723

**CERTIFICATE OF EXPRESS MAIL**

Express Mail Label Number EV 353609940 US  
Date of Deposit: July 2, 2003

I hereby certify that this correspondence is being deposited with the United States Postal Service "Express Mail Post Office to Addressee" service under 37 CFR 1.10 on the date indicated above and is addressed to Mail Stop PROVISIONAL PATENT APPLICATION, Commissioner for Patents, P.O. Box 1450, Alexandria, VA 22313-1450.

  
Candi L. Riggs

# Battery Float Management

The invention relates to a new VRLA battery float model. The model covers the steady state and transient float charge behaviour of both positive and negative electrodes. Backup analysis verifies the internal polarisation distribution for a conventional 2V-cell battery. This in effect encourages a virtual reference electrode where important polarisation behaviours can be identified without the need for a physical reference electrode. The estimated individual electrode polarisation allows early detection of common failure modes like negative plate discharge as well as a reference for float voltage optimisation. Furthermore the positive polarisation relating to minimum grid corrosion may be correlated with the occurrence of the peak of a 'Tafel' like resistance used by the model. The model encourages utilisation of low signal perturbation for testing a cell's state of health and state of charge conditions while at float.

## Potential Claim Structure

### 1 Group A: The battery float model

- The cell model is dominated by two dual-value capacitors that are serially connected
- One dual-value capacitor account for energy storage for each electrode (positive electrode and negative electrode)
- The two capacitor values of each dual-value capacitor relate to 1) the bulk energy storage, and 2) the overcharge capacitance.
- The model also features non-linear resistors that produce the 'Tafel' characteristics of each electrode. The peak in this positive 'Tafel' resistance appears to occur at the same positive polarization related to minimum corrosion level.

### 2 Group B: The electrode polarization

- Cell with a voltage above open circuit voltage when discharged present a compound voltage discharge profile
- The discharge could be due to open circuit charge leakage, or closed circuit enforced discharged
- Voltage measurement is made at the two external terminals of the battery without the use of reference electrode
- The polarization decay profile contains two main components. A fast and slow decaying transient components
- The slow decaying (hours of time scale) component is relevant to the positive electrode polarization. This is dominant in cells with float charge imbalance problems

- The fast decaying (minutes of time scale) is relevant to the negative electrode polarization. This may not be present in cells suffering with float charge imbalance problems

### 3 Group C: The application

- The total polarization applied to a cell is the difference between it's fully charged rest voltage and the float voltage (this is commonly accepted).
- The distribution of this applied total polarization between the positive and negative electrodes within a cell may be estimated through the magnitude ratio of the fast and slow components of the polarization decay. This polarization decay may be the natural open circuit decay or low rate forced decay (closed circuit)
- The presence or absence of negative electrode polarization could be sensed through injection of low frequency current perturbation into the battery cell.
- The frequency and injected signal level of the square wave type should be compatible with the negative electrode time constant.
- The rapid change in cell voltage as a result of the injected signal is dominated by a change in the negative electrode polarization
- Estimate of positive electrode polarization could be derived from the cell voltage before discharge and, the result of influence made by the injected signal
- Knowledge of the positive and negative electrode polarization is used in assessing the cell charge or health condition and may also be used to optimize the float voltage.

### Results

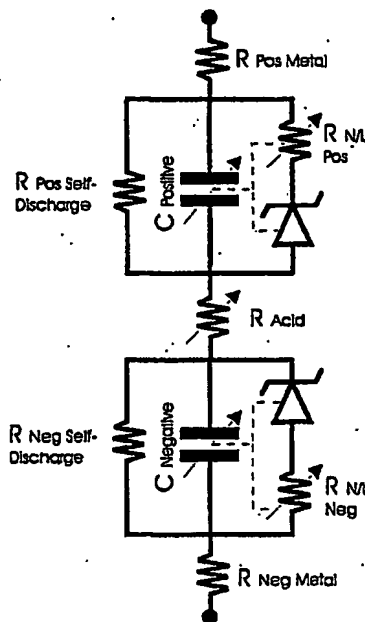
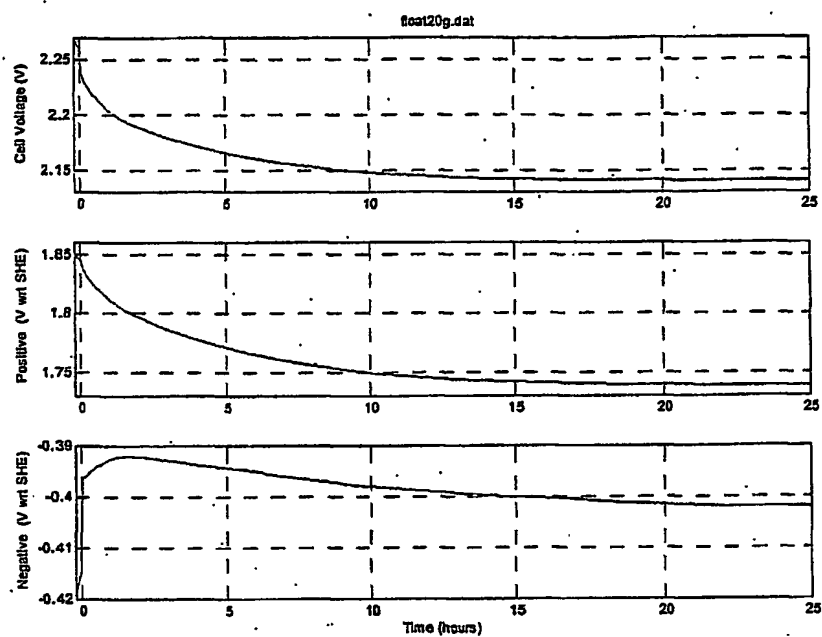
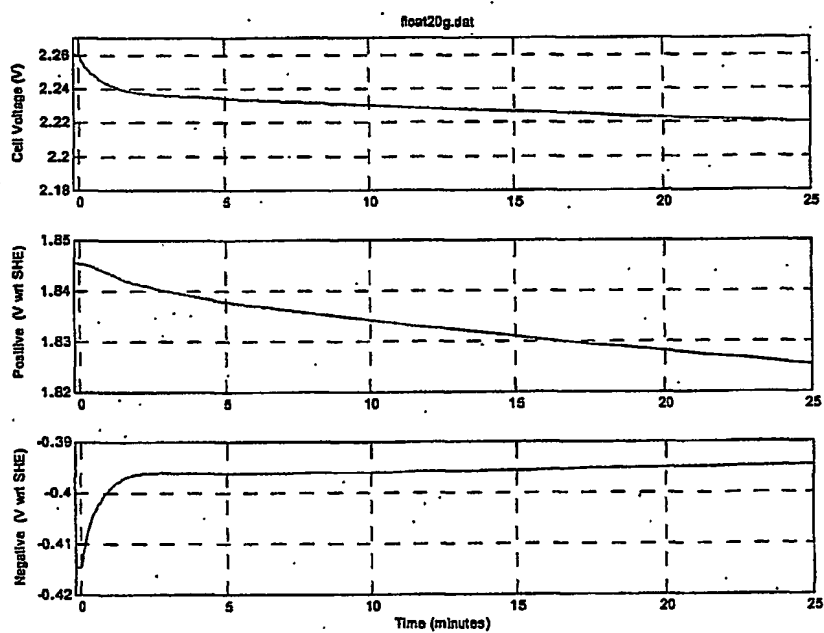


Figure.1 Implemented VRLA Battery Float Charge Simulation Model

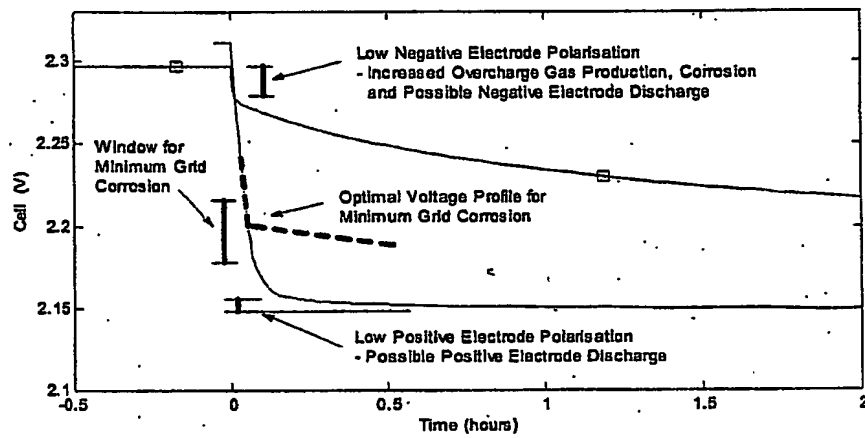
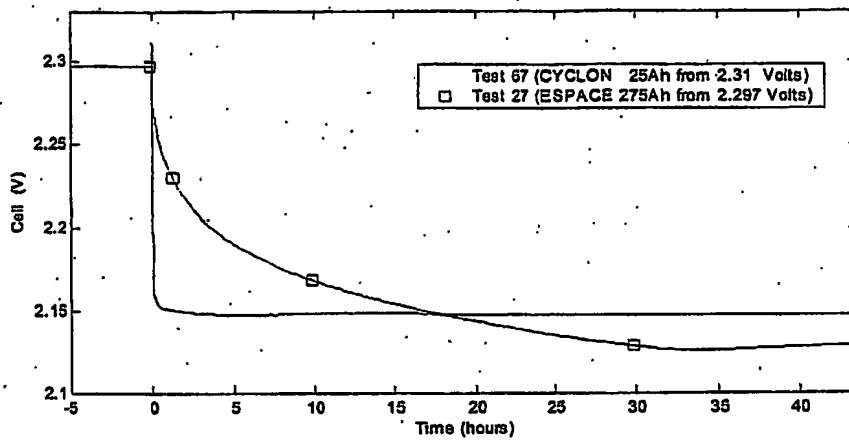


a) 25 Hours



b) 25 Minutes

Figure.2 Open Circuit 'Discharge' on Different Time Scales



## Battery float model

The approach is directly related to battery float management through modelling and sensing the battery positive and negative electrode contributions. Existing work/patents goes as far as adding additional hardware (related to electrochemistry like reference electrode .. etc.) into the battery in order to be able to sense the electrode contribution and hence perform control. The approach presented here does not require additional hardware. Electrode polarisation (battery internal parameters) could be sensed directly from the battery external terminals using a software procedure. This could be implemented through:

1. Open circuit test
2. Lowering the rectifier voltage to below open circuit voltage for short duration (see figure 1 below), or
3. Injecting a low frequency perturbation for short duration (see figure 2 below)

Knowing the status of electrode polarisation will help in identifying the state of charge and hence the required action to recover the balanced charge polarisation before any permanent damage could take place. It will also help in identifying any partial or full damage that has taken place through the successive charge/test procedures.

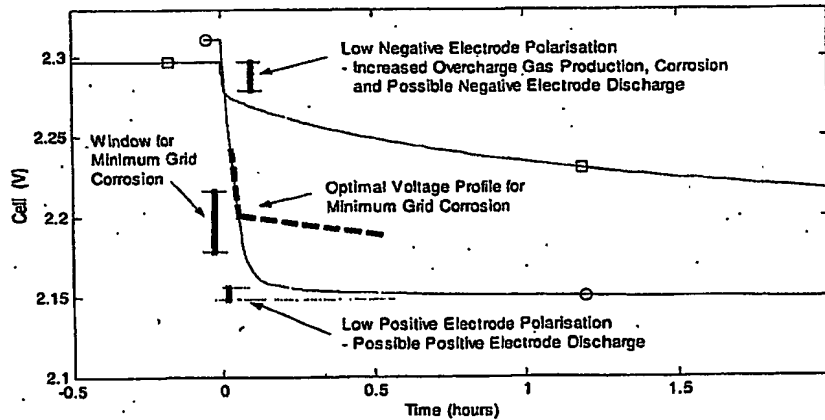
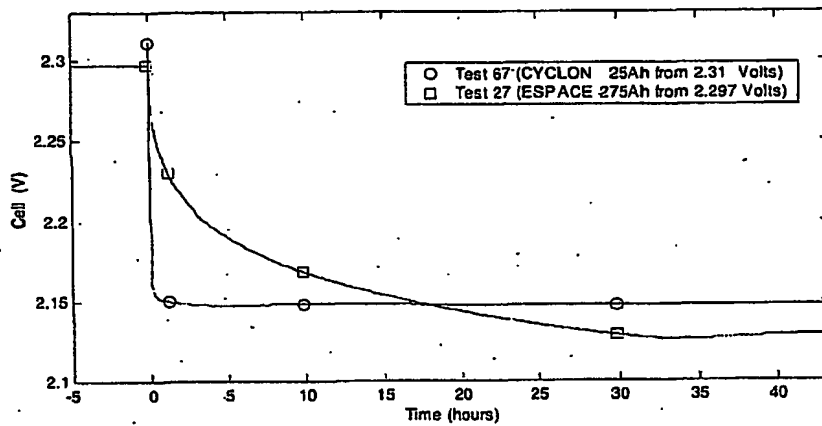


Figure 1 Low Negative, Low Positive, and Optimal Polarisation Discharge Profiles (Open Circuit)



## Decay

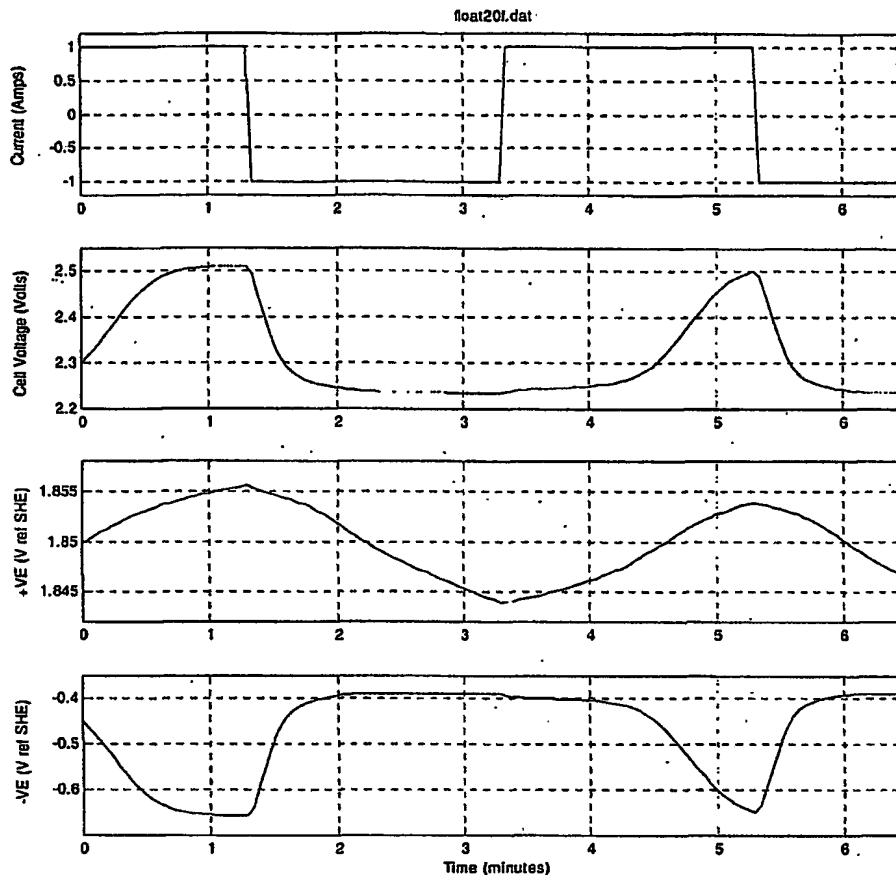


Figure 2 Response to  $\pm 1A$  perturbation

### Relevant Details

#### Sensed Polarisation Float Control

Successful and optimal float charging relies almost entirely on the distribution of polarisation between each electrode within a cell, and in particular, on the magnitude of the positive electrode's polarisation. To ensure optimal polarisations, several systems have been developed to sense or measure the electrode's polarisation<sup>1,10(21),iv</sup>. The measured results may then be used to appropriately adjust the float voltage, or current in order to achieve the desired polarisations. Of these systems, only the most recent<sup>iv</sup> describes control of VRLA batteries. This also suggests that the output voltage of the rectifier be adjusted so that the reference electrode to either the positive or the negative is set at a desired value.

#### Application

Two goals for float charge have been identified: 1) ensuring the battery remains fully charged, and 2) Maximising the life of the battery. Through appropriate distribution of the polarisation applied to the cell by the float charge, both of the identified goals of float charge may be realised simultaneously. However, the cell's design and construction largely determine the manner in which this applied polarisation is distributed within the cell. To a much lesser extent, the total polarisation applied to a cell may be controlled in an attempt to optimise the level of polarisation on individual electrodes within the cell.

Through modelling the steady state and transient characteristics of each electrode within a cell, a test and analysis technique has been developed that estimates the polarisation distribution within a float-charging VRLA cell. While the outcome of this test produces similar information to that obtained through reference electrode testing, the test does not use any form of reference electrode, and may be applied to any standard 2 V VRLA cell without any modification to the cell.

It is understood that many 'long life' VRLA cells suffer from low or no polarisation on the negative electrode. This mode of operation produces several mechanisms that impact on a cell's life expectancy. If the float voltage is not appropriately adjusted, the low negative polarisation will produce increased positive polarisation, thus raising the level of life-limiting positive grid corrosion, and also the rate of overcharge gas production. If gas production is excessive, gas venting and premature failure through dryout can result. Low or non-existent negative electrode polarisation may also result in a gradual discharge of the electrode to the point where the available capacity of the cell does not meet the load requirements, forcing replacement of the cell.

The problems that lead to the premature failure of some VRLA cells have been described in this work, and a simple field useable test and analysis procedure for identifying these problems and measuring the success of the applied float charge has been developed. As this work has focused on the identification of these float charge problems, and the development of an analysis procedure suitable for widespread field use, the strategies or techniques that may be used to attempt to correct problem cells have not been thoroughly investigated.

### Model Uses

The developed float charge model may have many alternative uses besides the intended assessment of cells on float charge in the field. Some of these uses may include provision of simulations for product development and testing, or tracking variations in a cell throughout its life by detailing variations in component values within the developed model. The latter suggestion may provide a timely indication that the end of battery life is imminent, allowing replacement batteries to be purchased prior to the battery failure occurring.

Due to the low voltage of a single VRLA cell, a number of cells are normally connected in series to form a 'string' in order to achieve useable voltages. As the string length is increased, the equalisation or uniformity of cell voltages tends to be reduced. To equal the 400 – 600 V DC provided by some UPS batteries, some two to three hundred 2 V cells must be series connected. The developed float charge model may also be serially stacked to simulate the operation of such long strings, however a slight spread will need to be specified for parameters such as float voltage, current, and polarisation. This spread in component values may be defined for best or worst case, or a random spread may be simulated within a specified window. With the modelling of a string of slightly different cells, battery-monitoring algorithms, string level optimisation, control techniques, and cell level equalisation methods and techniques may be simulated, assessed, and optimised.

If sufficient information is gathered during testing or general battery the model may be accurately calibrated for each cell. Over time, the unchanged model will highlight variations in the operational characteristics of the cell, as these change. Re-calibration of the model will highlight the components of the model affected by the changes in the cell. Depending on the model components that have altered, the cause of the change may be determined, and possibly linked to age, operation, or cell faults. However, as the developed model targets the float region of VRLA battery operation, in its present configuration some of the traditional failure modes, such as grid corrosion, may not be appropriately modelled. Further work is necessary to improve the model's representation of the bulk charge and discharge regions of operation if a complete assessment is required. The traditional (designed) cell failure mode is grid corrosion, which causes an increase in the internal resistance of the cell, and eventually limits the current that can be supplied by the cell for a given voltage drop. Internal resistance problems are best highlighted through high rate charge or discharge tests, as these high rate tests tend to be used to indicate capacity related state of health or remaining life. The developed test assesses the float operation of cells. The accuracy of this assessment improves as the discharge rate is reduced. As the best results are produced from open circuit decay, internal resistance does not have a large influence on the developed test. The developed model essentially assesses the SOC while the cell

is float charged. While it is understood that the float voltage variation between cells in the same string may be significant when the cells are new, this variation converges to a low value for the majority of the cell's useful life, and then diverges towards the end of life.

### **Test Procedure Uses**

The developed polarisation estimation test may have many applications besides the intended use of assessing cells in field service. The conventional method of assessing polarisation distribution in a laboratory involves the use of a reference electrode, however as a VRLA cell operates as a sealed unit, the addition of a reference electrode to a cell always has the potential to modify the cell's characteristics. It was seen in the first series of tests, using the ESPACE cell, that large variances in cell characteristics were produced through inconsistencies in the negative electrode Tafel line (intercept point). Atmospheric oxygen entering the cell through leaks in the case is said to have a depolarising effect on the negative electrode. Puncturing the cell's case to add a reference electrode must therefore increase the possibility of producing such leaks. As the developed polarisation assessment technique does not require any modification to the cell, the chances of altering the cell's characteristics must be reduced. The developed test may replace or supplement conventional laboratory reference electrode testing used during the development and design verification of new products. The polarisation estimation test may be extremely useful during accelerated life testing undertaken at elevated temperatures, where the use and maintenance of reference electrodes is difficult.

The developed polarisation estimation test procedure may also be used to verify the operation of cells after their manufacture, before they leave the factory. As newly manufactured cells are likely to have excessively wet separators, the paths through the separator required for oxygen recombination may not be fully developed. A new cell may therefore operate as a flooded cell until sufficient gas has vented, and the separator has dried to the point where recombination gas paths are developed. As flooded cells are expected to have well polarised negative electrodes, the absence of this may highlight electrolyte-filling problems, or possibly case sealing problems. The voltage decay profiles measured on cell terminals for open circuit or low rate discharges may be used to indicate product consistency.

### **Float Charge Optimisation**

Without knowledge of the polarisation distribution within a cell, any attempt to optimise the float charge must be based on historical data from other cells of similar type, generic empirical rules of thumb, or recommendations from laboratory based testing of the same cell type. As no simple or practical method of assessing the polarisation of standard cells was available, individual cell based float charge optimisation has not been possible.

Here a model of the float charge region of operation of a VRLA cell has been presented, and a test and analysis technique has been developed to provide an estimate of the polarisation distribution within any standard 2 V VRLA cell. While this model was essential for the development and verification of the test and analysis technique, a calibrated model is not essential for analysis of a cell's polarisation. The developed testing technique requires only the cell's polarisation decay profile for polarisation estimation.

As the majority of this work has focused on developing the tools necessary to obtain polarisation estimations, little work has been undertaken on optimisation techniques and strategies to ensure both float charge goals are achieved. For a well designed cell that displays consistent textbook Tafel characteristics, the optimisation should be simple and uncomplicated. However with cells identified to be suffering from electrode polarisation problems (either positive or negative), the optimisation may be more complicated. The two cells extensively tested in this thesis were both shown to have poor electrode polarisation distributions. When the float voltage was varied on both of these cells, unexpected redistribution of the applied polarisation resulted.

It is believed that a large number of VRLA cells in field service suffer from electrode polarisation problems, the most predominant of which is negative electrode discharge. Further work is required to determine appropriate control strategies to that ensure the cell is maintained in a fully charged state, and that maximum life for the defective cell is realised. For example, two courses of action may be available should a cell be proven to be suffering from a gradual discharge of the negative electrode. It must be determined whether it is more beneficial to: a) raise the float voltage in an attempt to polarise the negative electrode, at the expense of increased positive grid corrosion and possible dryout resulting from gas venting, or b) reduce the float voltage, giving the positive electrode optimal polarisation for

minimal grid corrosion, and perform regular boost charges to ensure that the negative electrode is periodically fully charged.

When cells are charged in a series string, a spread in the terminal voltages of individual cells is often seen. The developed polarisation estimation technique may be used to assess the benefits or disadvantages of various cell voltage equalisation schemes. The advantages of natural voltage (no equalisation), uniform voltage equalisation, and optimal voltage for each cell using individual positive polarisation values may be compared to determine the scheme that best fulfils the float charge goals for the entire string.

Temperature compensation is a common technique that is used when cells are operated at temperatures either higher or lower than the designed operating point. While temperature compensation may reduce overcharge gas production levels and the possibility of thermal runaway, it does not maintain an optimal polarisation for minimum grid corrosion. Because the developed polarisation estimation assessment technique is unaffected by temperature, the polarisation at the compensated float voltage may be assessed following initial application of the recommended temperature compensation. This will determine whether the float voltage is appropriate, and whether the goals of float charge have been achieved.

Conventionally, a specific single float charge voltage is recommended for a given cell type, regardless of its age. The developed polarisation assessment technique will allow an optimal float voltage to be maintained throughout the life of the cell. This may compensate for cell characteristic variations due to age, or operational history. Further work would be required to assess the advantages or disadvantages of such an optimisation system.

A simple tool has been developed to provide an assessment of the polarisation distribution within any standard 2 V VRLA cell. With the information provided by this test, many float charge optimisation schemes may be assessed and compared. The developed tool will identify cells with float charge problems before permanent damage is done, and also provides a measure of the success of the float charge, allowing the effectiveness of any correction or optimisation techniques to be assessed. As a tool is now available to assess the operation of VRLA cells on long term float charge in field service, float charge problems may be identified promptly. This allows corrective action to be taken in the early stages, before the problems escalate to levels where unrecoverable damage is sustained by the cell.

### **Technical Development**

A continuous power supply is critical to the success of many applications. Telecommunication systems are a prime example of this, as they are expected to function continuously in the event of a power outage. A typical telecommunication power system converts the AC-grid power to 48 V DC, and then uses this to charge storage batteries and supply the load. In the event of a disruption to the AC-grid power, critical plant is supplied directly from the storage batteries. Depending on the load size and required backup time, large amounts of energy storage are often necessary. Lead acid batteries are traditionally used as the storage element due to their relatively low cost, high energy density, and reliability. However there has been a recent trend towards the use of Valve Regulated Lead Acid (VRLA) batteries due to perceived savings from reduced maintenance and ventilation requirements. The chemistry of a VRLA battery is the same as a conventional flooded lead acid battery, but the physical construction of a VRLA cell has been optimised to allow the gases produced during overcharge to be recombined back into water. Periodic addition of water to replace that lost through gas venting is therefore not required (or possible) with a VRLA battery. In situations where there is a reliable AC power supply, years can pass before the power supply might be interrupted, during this time the storage batteries must be maintained in a fully charged state. All lead acid batteries have a natural self-discharge, so a float charge must be supplied in order to maintain the battery in a fully charged state. Constant voltage float charge is normally recommended, and may be specified as a function of the battery temperature.

Through this research, the goals of optimal VRLA battery float charge management are identified, and the requirements for measuring or verifying the achievement of these goals are also established. An investigation into the problems associated with present float charge methods and existing float charge optimisation and analysis techniques is also undertaken. The problems and suspected mechanism

leading to the premature failure of some 'long life' VRLA batteries is described, and a test procedure for the early detection of this failure mechanism is developed. Analysis of the developed test procedure, applied to the terminals of a standard 2 V VRLA cell, provides an estimation of the polarisation distribution within the cell. As the procedure reveals information that traditionally could only be obtained through the careful use of an additional reference electrode, the test and analysis may be used as a virtual reference electrode for float optimisation. An equivalent electrical model of the float charge region of a VRLA battery is also developed. This model reproduces both the steady state and transient responses of a VRLA cell on float charge.

Two goals of float charge have been identified:

- 1) Ensure the battery remains fully charged indefinitely.
- 2) Maximise the life of the battery by maintaining ageing effects at minimum levels.

To ensure that a cell remains fully charged, both electrodes within the cell must be sufficiently polarised (raised above their fully charged open circuit rest-potential). To maximise the life of a VRLA cell, grid corrosion and gas loss (venting) must be minimised. The traditional (designed) failure mechanism of lead acid batteries is excessive corrosion of the positive grid. The grid forms a low resistance path within the electrode, allowing large currents to be drawn from it. Grid corrosion reduces the cross-sectional conductor area, which increases its resistance. Eventually this resistance rises to a point where the cell can no longer supply the necessary current at the required terminal voltage. At this point the cell is said to have reached the end of its life. Due to the potentials involved, positive grid corrosion can never be completely eliminated, but it can be optimised to ensure the lowest possible rate. It is commonly accepted that the rate of positive grid corrosion is a function of the polarisation on the positive electrode, and has a minimum rate occurring at a polarisation slightly greater than the open circuit rest potential. While there is some debate on the actual voltage at which the grid corrosion minima occur<sup>vi, vii</sup>, a window of acceptable grid corrosion occurs between 40 and 80 mV. The polarisation associated with minimum grid corrosion may vary with cell chemistry.

A typical fully charged open circuit rest voltage for a VRLA cell is 2.14 V. For such a cell a float voltage of 2.27 V may be recommended. At this float voltage, a total polarisation of 130 mV must exist. If, for example, the optimal positive electrode polarisation for minimum corrosion exists at 50 mV, the negative electrode must then support the remaining polarisation of 80 mV. As both electrodes are raised above their open circuit potentials, the primary goal of float charge will also be satisfied, and the cell will be maintained in its fully charged state indefinitely.

Traditionally, an optimal (recommended) float charge voltage is determined on sample cells in a laboratory with the aid of a reference electrode. This recommended float voltage is then applied (largely unchecked) to cells in service in the field. A further complication is that 2 V cells are connected in series to produce the desired system voltages (typically 24 or 48 V). A single supply is then used to charge the series connected cells. Small differences between cells (resulting from manufacturing variance) may produce a distribution of cell voltages, despite all cells receiving an identical float current due to the series connection.

With an industry trend towards reducing battery maintenance, longer life batteries are desirable. However it is becoming increasingly apparent with many 'long life' VRLA batteries that either, poor design or, poor quality manufacturing results in the cells failing prematurely in the field. This is believed to be due to internal electrode balance problems, and in particular negative plate discharge. As grid corrosion is the traditional failure mechanism, an obvious way to improve the battery life is to reduce the rate of grid corrosion. This may be achieved by altering the grid alloy. However for balanced float charge operation, the current associated with corrosion of the positive grid, must balance the current associated with (impurity related) hydrogen evolution at the negative. If the grid corrosion rate is reduced and the purity of the negative electrode is not appropriately increased, polarisation of the negative electrode must decrease to supply current for hydrogen evolution. If the current associated with hydrogen evolution at the negative electrode is sufficiently large when compared to the current consumed through positive grid corrosion, the entire applied polarisation will be supported by the positive electrode. A gradual discharge of the negative must result in order to supply the current required for hydrogen evolution. While this rate of negative electrode discharge is extremely low, the cumulative effects over months or years of float charge can be significant. Furthermore, as the applied polarisation is supported entirely by the positive electrode, increased rates of grid corrosion, gassing, and possible dryout must result.

Analysis and subsequent optimisation of the float charge relies heavily on knowledge of the polarisation distribution between the positive and negative electrodes within a cell. Conventionally, an optimal float voltage is determined by the cell manufacturer and is applied virtually unmonitored to all cells of that type in field use. However, due to the importance polarisation plays in float charge optimisation, a number of schemes have been published<sup>viii,ix,x,xl</sup> that use varying designs of reference electrodes or reference cells for float polarisation analysis and subsequent control purposes. Without exception, all of these systems require cell modifications to facilitate the use of the reference electrode or reference cell. As VRLA cells basically function as a sealed unit, it is difficult to insert a reference electrode without disturbing the seal and modifying the cells' characteristics.

A test and analysis procedure has been developed to produce an estimate of the distribution of polarisation between the positive and negative electrodes within a cell. This test is applied to the terminals of a conventional 2 V VRLA cell, and no reference electrode or cell modifications are required. Provided the battery is properly designed and manufactured, optimal float charge requires the polarisation on the positive electrode to be maintained within a defined (minimum corrosion) window. The estimated polarisation distribution may be used to determine whether the test cell is fully charged, and if so, how optimal the float voltage is. It can also be used to determine whether the test cell is suffering from imbalance problems, such as positive or negative plate discharge. In effect, the test and analysis procedure produce a virtual reference electrode, as information on the polarisation of each electrode is obtained. The test can be performed with only a small amount of low-power electronic hardware. The size and cost of this hardware lends itself well to automated field use. Based on significant differences in the transient decay of the polarisation on each electrode, the test requires only cell terminal voltage measurements and a low-rate constant current discharge (of a similar magnitude to the normal float current). With a typical test duration being less than ten minutes, the test has negligible impact on cell health, as the depth of discharge is typically less than 0.01%.

With the aid of a reference electrode, a thorough investigation of the float charge characteristics (steady state and transient) of a VRLA battery has been undertaken. The results of this testing have allowed the development of an equivalent electrical model of each electrode to be produced. For an applied current, the developed electrode models reproduce the voltage response seen at both electrodes within a cell, or, for an applied voltage, the models will draw the correct current. Combining the models of the positive and negative electrodes reproduces the overall terminal response of the cell.

While the electrical-equivalent model has not been developed to represent chemical reactions occurring within a cell, the physical layout of the model is linked closely with the physical construction of a cell. The model's component values and transition points may be interpreted as features of the chemical reactions, however the model is not based on, or intended to represent, the actual chemical processes occurring within a cell. As the target region of battery operation is at or near float charge, to avoid confusion and minimise calibration requirements, the model's representation of the bulk storage is limited. Should a complete battery model be required, further investigation and development of the bulk charge storage region will be necessary.

Although the developed float charge model is not strictly required for the developed polarisation estimation test and analysis, it does simplify the understanding of the processes occurring within a cell. This may be beneficial if the present float charge operating point is to be used as a basis for further optimisation of the float charge voltage. There are many other applications that may benefit from the developed VRLA battery float charge model. Such applications may include a battery simulator to aid the development, optimisation, and modelling of cell equalisation hardware, or the overall control of the power system. Battery chemists and manufacturers may also benefit from the float charge model and the polarisation estimation test, as non-intrusive verification testing may be performed on new and existing products. The float model may provide a simple method of tracking or characterising the internal operation of a cell during natural or accelerated ageing. Furthermore, the float charge model and associated polarisation estimation test may be used to determine the internal characteristics (Tafel plots etc) of cells that have been identified as problem cells during field-testing. With knowledge of the actual root of the problem, the most appropriate corrective action may be taken.

## References

- <sup>i</sup> E. A. Willihnganz, *Method and Apparatus for Measuring the State of Charge of a Battery Using a Reference Battery*, US Patent 3,657,639, April 18 1972.
- <sup>ii</sup> Y. M. Mistry, T. D. O'Sullivan, *Electrical Storage Cell Life Extender*, US Patent 4,935,688, June 19 1990.
- <sup>iii</sup> T. D. O'Sullivan, C. F. Leung, *Field Test of the Polarisation Controller on a Mixed Battery String*, Proceedings of INTELEC 1992, 9-1.
- <sup>iv</sup> S. C. Chalasani, V. J. Thottuvelil, *Recharging Circuit and Method for Recharging a Battery Having a Reference Electrode*, US Patent 6,137,266, October 24 2000.
- <sup>v</sup> D. Berndt, U. Teutsch, *Float Charging of Valve-Regulated Lead-Acid Batteries: A Balancing Between Secondary Reactions*, Journal of the Electrochemical Society, Vol. 143, No. 3, March 1996.
- <sup>vi</sup> J. Jergl, B. Cole, & S. Purcell, *Real World Effects on VRLA Batteries in Float Applications*, 11-4, INTELEC 1996.
- <sup>vii</sup> W.B. Brecht, D.O. Feder, J.M. McAndrews, A.J. Williamson, *The Effect of Positive Polarisation on Grid Growth, Cell Performance and Life "Willihnganz Revisited – 20 Years Later"*, 5-7 INTELEC 1988.
- <sup>viii</sup> S. C. Chalasani, V. J. Thottuvelil, *Recharging Circuit and Method for Recharging a Battery Having a Reference Electrode*, United States Patent 6,137,266, October 24, 2000.
- <sup>ix</sup> T. D. O'Sullivan, C. F. Leung, *Field Test of a Polarisation Controller on a Mixed Battery String*, 9-2 INTELEC 1992.
- <sup>x</sup> K. M. Mistry, T. D. O'Sullivan, *Electrical Storage Cell Life Extender*, United States Patent 4,935,688, June 19, 1990.
- <sup>xi</sup> E. A. Willihnganz, *Method and Apparatus for Measuring the State of Charge of a Battery Using a Reference Battery*, United States Patent 3,657,639, April 18, 1972.

### Additional Information

Figure 1 illustrates a simplified diagram of the float electric model together with the relevant battery electrodes representation. Both charge polarisation capacitor and leakage resistor are represented. The polarisation contribution and discharge transient are key to the representation. Traditionally this information is only obtained through inserting a reference electrode (see figure 2). Chalasani of Tyco in a publication (year 2000) suggested inserting additional electrode running in parallel to the main electrodes for capturing the information. The solution in both cases is to insert additional elements to the battery that could result in disturbing the battery characteristics and incurring additional cost.

The patent suggest a software model that helps identifying the key polarisation information required to manage the battery during float without the need for inserting additional physical element into the battery. The tools will substantially help managing the battery float voltage throughout the various stages of battery life. Resulting in reducing the associated stress and hence prolonging the operational life.

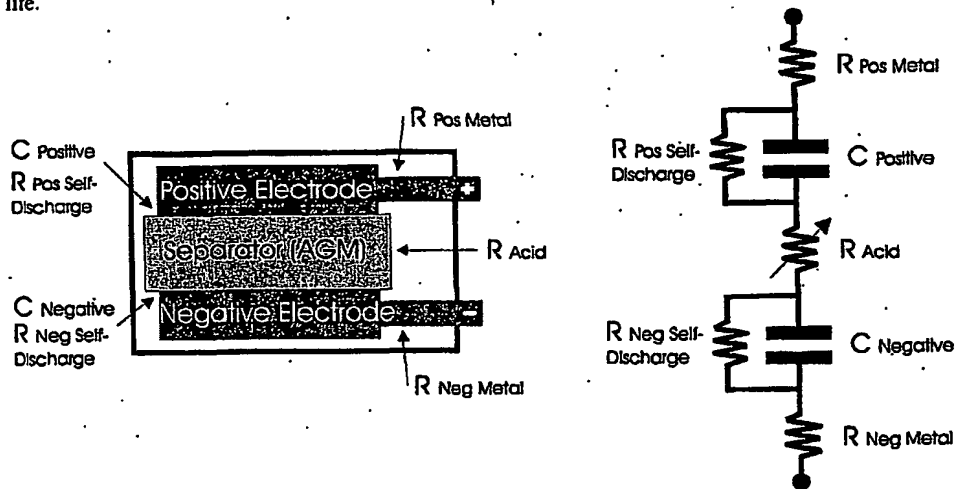


Figure 1

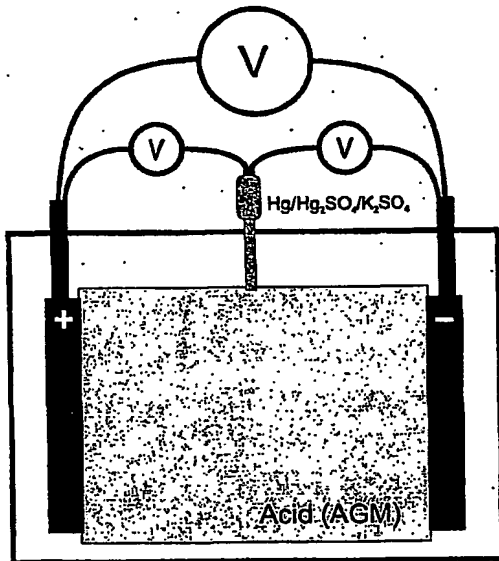
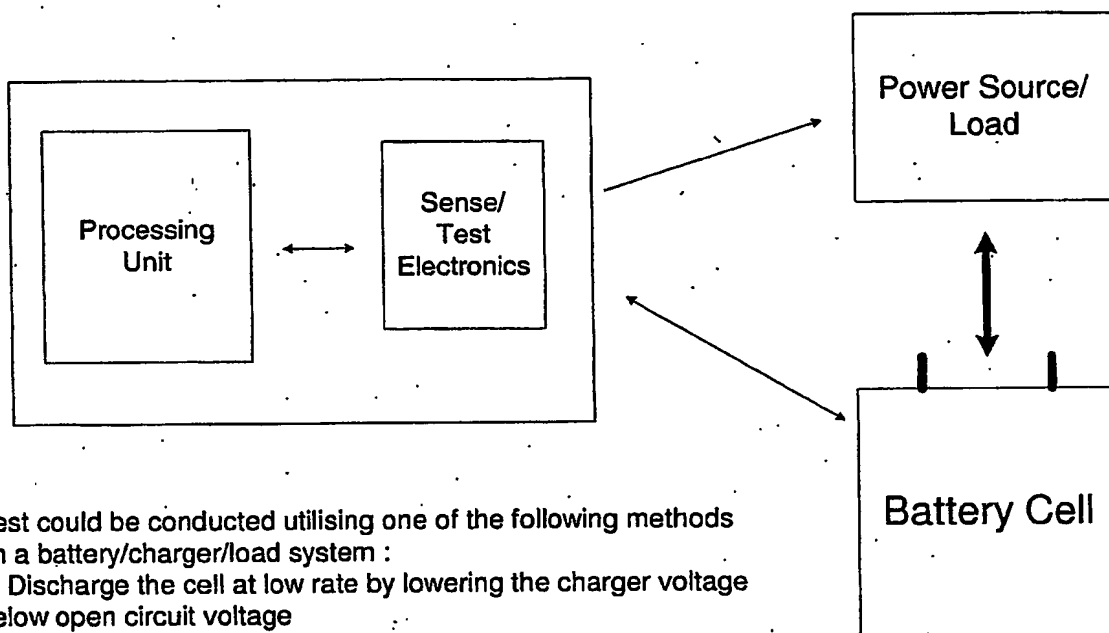


Figure 2





Test could be conducted utilising one of the following methods on a battery/charger/load system :

1. Discharge the cell at low rate by lowering the charger voltage below open circuit voltage
2. Open circuit the cell and self-discharge
3. Introduce a perturbation by the test electronics through the sense line

performed on single cell

Processing unit could play one or more of the following roles:

1. Capture the discharge transient and present it to the operator for analysis of electrodes polarisation contributions
2. Capture the transient, perform analysis to the polarisation contribution and report abnormal conditions based on current conditions and model knowledge.
3. Capture the transient, perform analysis to the polarisation contribution, calculate and recommended float implementation.
4. Workout the float settings for peak positive polarisation resistance. This could prove to be the most appropriate float setting for minimum corrosion.

# 1 Model Implementation

The float charge model was developed to allow steady state and transient float charge features of both electrodes to be modelled. While the components and their layout have been selected to reproduce the overcharge response and aid understanding of float charge operation, simulation of this model is complicated by the two switches that short (eliminate) the overcharge components. With two switches, four ( $2^2$ ) separate simulation circuits are required so that all combinations of switch states are represented. On-Off switches do not allow smooth transitions to be made from one state to the next. Replacing the switches with variable resistors that change from a short (zero-ohms) to open circuit (meg-ohms) may provide smooth transitions. However zero-ohm resistors pose computation problems (divide-by-zero errors), as circuit nodes have effectively been eliminated. For simulation simplicity the model has been simplified to that shown in Figure 1.1. The dual capacitors representing the bulk and overcharge capacitance of each electrode have been combined into a single variable capacitance which 'switches' between the bulk and overcharge values. A smoothly transitioned switch may be achieved through implementation of appropriate mathematical function.

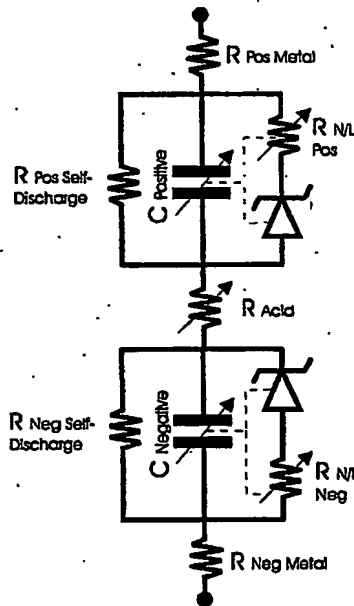


*Figure 1.1 Implemented VRLA Battery Float Charge Simulation Model*

## 1.1 Model Components

Matlab and the Matlab Ordinary Differential Equation (ODE) solver were chosen as the environment for the development and simulation of the VRLA battery float charge model shown in Figure 1.1. While it should be possible to simulate the cell model in any electrical circuit simulation package, modelling of non-standard components such as the non-linear (logarithmic) overcharge resistors and the dual value capacitors may be difficult to implement in some of these packages. Matlab provides an environment that does not have any limitations on how components are specified. Component values may be specified as functions of other components, or as functions of the present state (voltage-across or current-through) of other components in the circuit. Similarly, piece-wise modelling can be implemented through the use of 'if - then' statements. This is useful for implementing components such as zener diodes.

The software is broken into three components: component sizing, model equations, and simulation control. In the remainder of Section 1.1 the individual components of the model are described, along with how appropriate values were selected.

### 1.1.1 Non-Linear and Self-Discharge Resistors

As a Tafel plot represents the steady state characteristic, no net charging or discharging of the cell exists. Virtually all of the energy supplied to the cell through the float charge is consumed in the internal gas cycle. Eventually, this energy must either be dissipated to the atmosphere as heat, or lost through gas venting. As there is no net change in stored energy during steady state float, resistance is the obvious choice of model component. However, the straight lines of a Tafel plot are produced only when a linear/log graph is used to plot polarisation against float current. This suggests that a single or constant value resistor is not appropriate. The resistance value required to replicate Tafel characteristics must be a function of either the electrodes' polarisation, or the applied float current. The top left plot of Figure 1.2 shows a single Tafel line that has a slope of 100 mV per decade, and a polarisation of 250 mV at a float current of 1 A. In the lower plot of Figure 1.2, the variation in resistance required to produce the Tafel line is shown as a function of float current, while in the right hand plot of Figure 1.2 the required resistance is plotted as a function of the electrodes' polarisation.

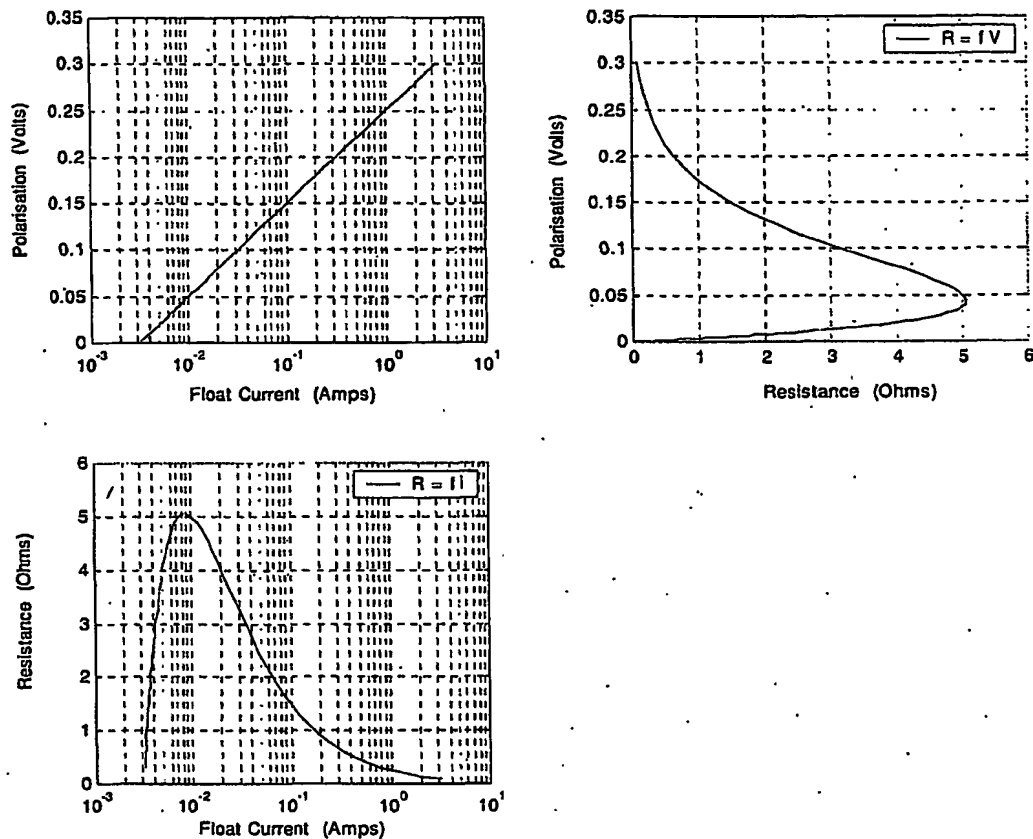


Figure 1.2 Equivalent Overcharge Resistance as a Function of Float Current or Polarisation

A Tafel line may be specified through any two of the following: 1) Tafel intercept (current at zero polarisation); 2) Tafel slope; or 3) Polarisation at a point (e.g. 1 A). The relationships between these points are graphically shown in Figure 1.3. The component value selection program `vrla_part_size.m` uses the specified float voltage, the float current, the polarisation of the positive electrode at the float voltage, the open circuit voltage, and each electrode's Tafel slope to calculate the polarisations of each electrode at 1 A. By doing this, the location of the positive Tafel line is directly defined by the specified operating point. The location of the negative Tafel line is used to balance the equations concerning the total polarisation supplied to the cell at the float voltage. Figure 1.3 shows the relationship between the possible variables used to describe a Tafel line and how the required simulation parameters are obtained by the software `vrla_part_size.m`. The

simulation model required the parameters shown in **bold** (Tafel slope and polarisation at 1 A), while the characterisation (specifying) parameters are shown in *italics*. Experience has shown that the location of the positive Tafel line is reasonably stable over time, however the location of the negative Tafel line has been seen to drift considerably. The Tafel slopes of each electrode have also been seen to remain reasonably consistent over time.

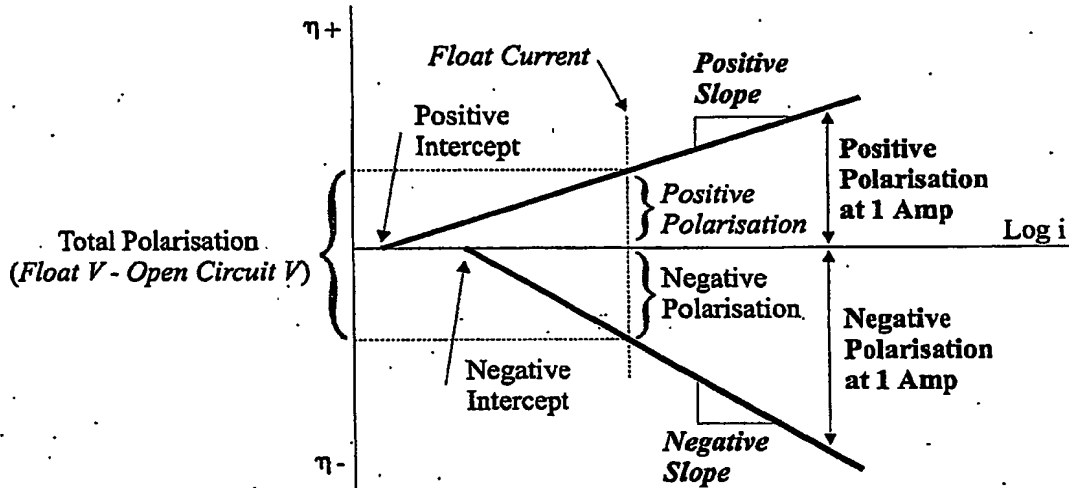


Figure 1.3 Model Specification of the Overcharge Tafel Characteristic

Equation 1) shows how the non-linear overcharge resistance is calculated as a function of the polarisation voltage (difference between the capacitor and zener voltages) and the model parameters (polarisation at 1 A and Tafel slope). This function may be easily scaled to represent any desired Tafel line, and was used to produce the polarisation versus resistance curve shown in Figure 1.2. Experimental polarisation data may show a slight deviation from a straight Tafel line, especially at low polarisation values. While for most purposes a straight Tafel approximation is satisfactory, if a more precise simulation is necessary Equation 1) may be modified as required.

$$r = \frac{p}{10^{\left(\frac{p-p1}{s}\right)}} \quad 1)$$

where:  $r$  = resistance

$p$  = polarisation (volts)

$p1$  = polarisation at 1 A

(volts)

$s$  = Slope (volts / decade)

The value of the self-discharge resistor is selected so that the minimum current required for polarisation (Tafel intercept) is drawn at the point when polarisation begins, i.e.:

$$R_{\text{Self-discharge}} = \text{zener\_voltage} / \text{Tafel\_intercept\_current} \quad 2)$$

Subtracting the capacitor voltage from the diode's zener voltage produces the electrode's polarisation. Ohms law is then used to calculate the current flowing through the non-linear (overcharge) resistor based on the polarisation and the resistance value. Similarly, the capacitor voltage and the self-discharge resistance are used to calculate the self-discharge current. Figure 1.1 shows the self-discharge resistor in parallel with the series connected overcharge resistor and zener diode combination. This is not entirely correct, as the self-discharge resistor should be in parallel with the zener diode. It has been implemented as shown in Figure 1.1 however, in order to avoid computation problems. At and below the fully charged open circuit voltage, the non-linear overcharge resistor must have no resistance, however this introduces divide-by-zero computation problems. To compensate for the current through the self-discharge resistor during overcharge, this self-discharge current is subtracted from the overcharge resistor current before the differential equations are solved.

#### 1.1.1.1 Minimum Grid Corrosion Point – An Observation:

In Figure 1.2 a voltage- or current-dependant equivalent resistance that replicates Tafel characteristics is shown. While the computation of this equivalent resistance may be achieved with a simple Ohms law calculation at each steady state operating point (voltage-current pair), plotting this equivalent resistance against current or voltage reveals an interesting characteristic. It can be seen in the top right plot of Figure 1.2 that there is a peak in resistance at approximately 43 mV. The corresponding Tafel line has a slope of 100 mV per decade and 250 mV of polarisation at 1 A. Interestingly, the peak in resistance occurs within the accepted window (40 - 70 mV) for minimum grid corrosion. While this is purely an observation derived from a mathematical phenomenon, it does entice further investigation.

Figure 1.4 shows the corrosion current versus electrode potential for several lead alloys by several experimenters. While it is acknowledged that the various tests were performed under differing

conditions with different techniques, and that direct comparisons can therefore not be made, general trends can be identified. For reference, a Tafel slope of 80 mV per decade has also been shown for oxygen evolution. It can be seen that the Tafel slopes for the corrosion of lead and lead alloys vary from 170 mV per decade (Rogatchev (1983) 10.6%) to 255 mV per decade (Willihnganz).

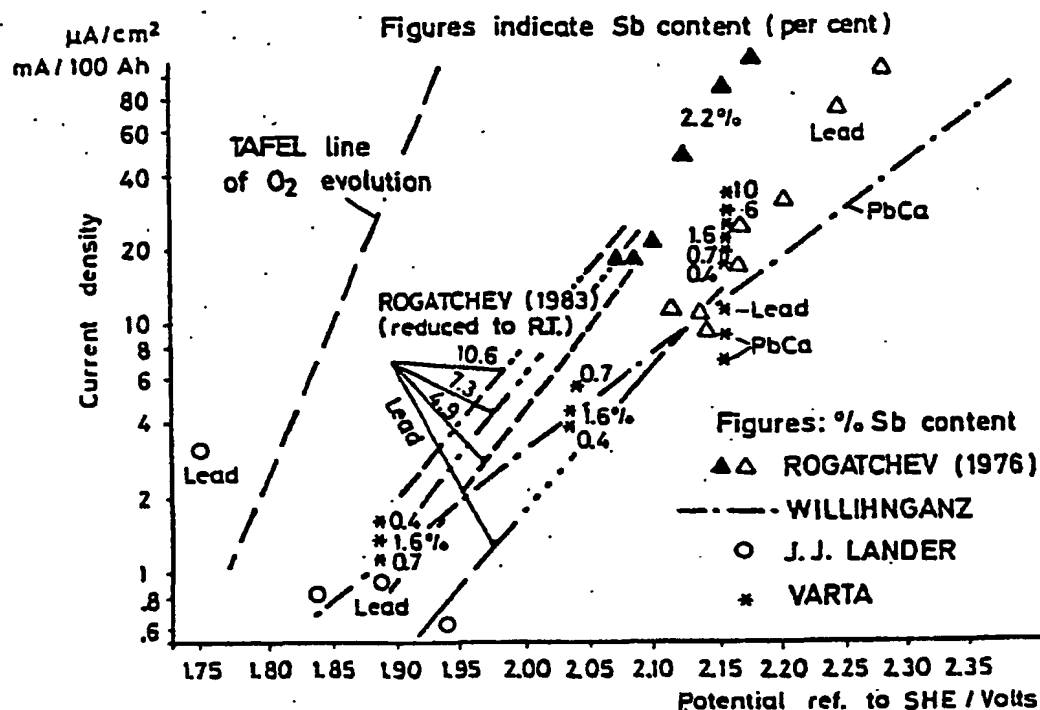
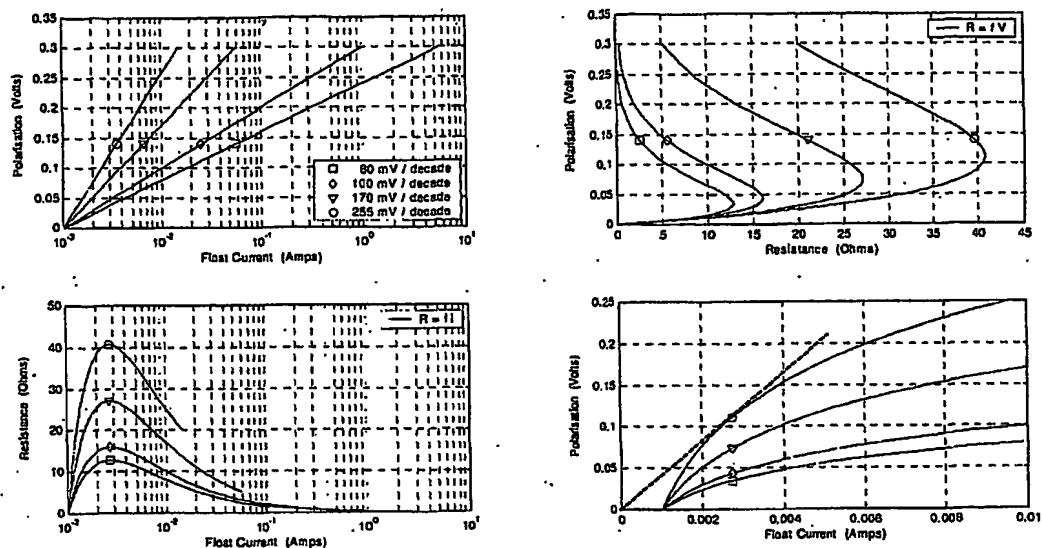


Figure 1.4 Corrosion Rate of Lead and Lead Alloys at Constant Potential<sup>1</sup>

Corrosion is a complex reaction, influenced by external parameters such as temperature, electrode potential, and acid concentration, as well as by internal parameters including the composition of the corroding alloy, metal lographic structure, and local distribution of alloying additives. Corrosion rate measurement must be based on a number of general rules combined with empirical experience, as exact evaluation may not be possible<sup>1</sup>. However the observation detailed below, based on the characteristic of the electrode as a whole, displays some interesting features and similarities to experimental data.



*Figure 1.5 Variation in Equivalent Resistance with Tafel Slope*

Figure 1.5 compares the Tafel slopes for oxygen evolution and the corrosion rates of several lead alloys shown in Figure 1.4. The Tafel lines have all been normalised to have a zero polarisation intercept point at 1 mA. The equivalent resistances required to replicate the Tafel lines have been calculated and plotted against polarisation (top right), and float current (bottom left). The equivalent resistance versus float current plot shows that the current associated with the peak in equivalent resistance remains constant regardless of the Tafel slope. However the polarisation at which the equivalent resistance peak occurs increases with the Tafel slope.

When a linear axis is used to plot the polarisation-voltage/float-current data, the reason for the occurrence of the peak in the equivalent resistance becomes apparent. The same polarisation versus float-current data shown in the top left plot of Figure 1.5 has been re-plotted in the lower right plot on a linear axis. With a conventional fixed value resistor, current is a direct function of the applied voltage, and a voltage-current plot of such a resistor will pass through the origin. The bold line in the lower right plot of Figure 1.5 shows that the point at which a line starting at the origin forms a tangent with the polarisation-current curve corresponds to the peak in the equivalent resistance. At polarisations lower than this tangent point, the curve has a steeper slope, indicating



increased resistance, while at polarisations above this tangent point, decreased resistance is indicated by a gradient lower than the fixed resistance.

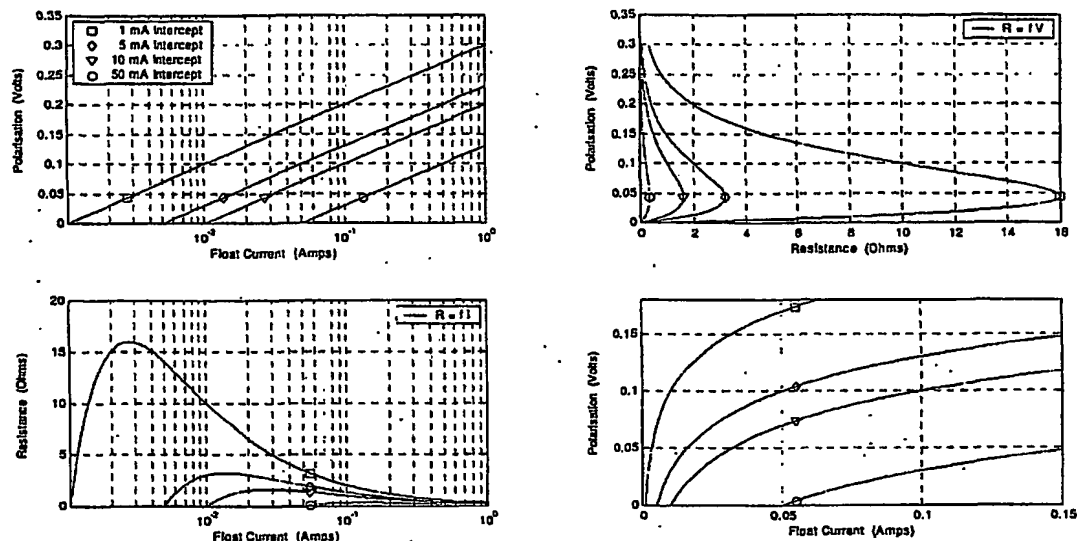


Figure 1.6 Variation in Equivalent Resistance with Intercept Point

Figure 1.6 shows four Tafel lines with an identical slope of 100 mV per decade, separated by differences in the zero polarisation intercept point. It can be seen in the plot of equivalent resistance versus polarisation that despite the differing Tafel intercept point, the polarisation at which the peak in resistance occurs remains constant. The plot of the float current versus equivalent resistance shows that the float current at which the peak resistance occurs increases in association with the zero polarisation intercept point.

The Tafel slope determines the polarisation at which the peak in equivalent resistance occurs. The current of this peak is determined by the current at which the zero-polarisation intercept point occurs. In batteries of differing capacities, the float current is expected to increase proportional to the capacity. A Tafel plot of the positive electrode's polarisation would however have the same slope regardless of the cell's capacity. As the Tafel slope remains constant, the polarisation at which the peak in the equivalent resistance occurs would also remain constant.

As the lowest Tafel slope (i.e.: oxygen evolution) dominates the polarisation of the electrode by consuming the most current to support the reaction, the significance of the Tafel plots relating purely to the rates of grid corrosion is reduced. The overall polarisation of the electrode is set through the dominant reaction of oxygen evolution. The current consumed through grid corrosion is determined by the polarisation on the electrode rather than by the current flowing through it. Therefore, as the float current is increased, the change in current consumed through grid corrosion is significantly reduced from that expected by the corrosion Tafel line, despite the grid corrosion Tafel plots having a greater slope.

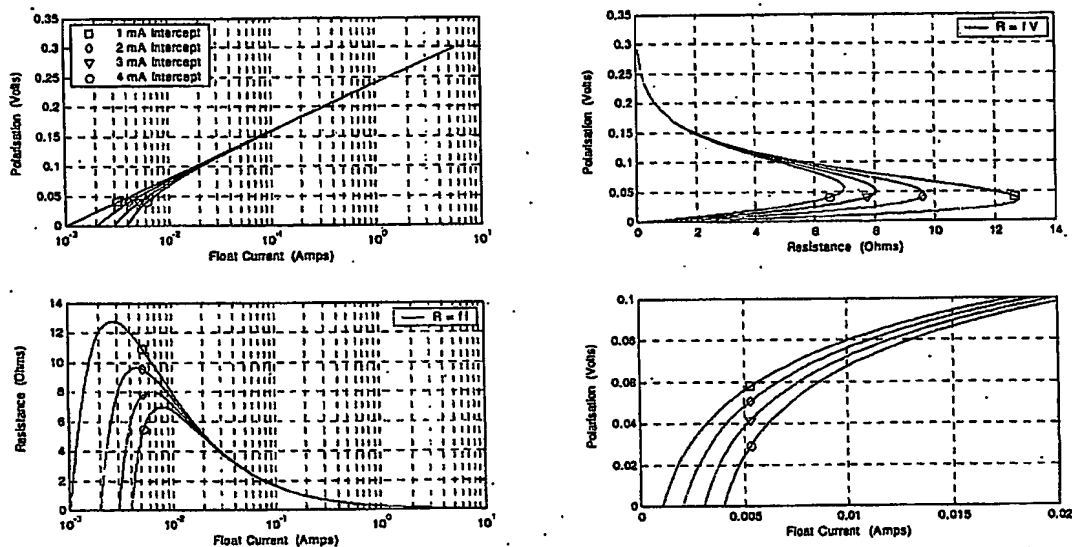


Figure 1.7 Variation in Equivalent resistance with Grid Corrosion Correction

Figure 1.7 shows the effects of adding grid corrosion currents of 1, 2, and 3 mA to an 80 mV per decade, 1 mA intercept, Tafel line representing the evolution of oxygen. The introduction of a slight curve can be seen at low polarisations, as the corrosion current becomes significant in comparison with the oxygen evolution current. The increase in corrosion current required to produce an increase in polarisation is insignificant when compared to that associated with oxygen evolution. For this reason, Tafel plots are often simplified to a straight line associated with oxygen evolution, rather than the slight curve seen at low polarisations.

The curved traces in the top left plot of Figure 1.7 are characteristic of that expected for the positive electrode (combining oxygen evolution and grid corrosion) in a VRLA battery. Interestingly, the equivalent resistance versus polarisation plot, seen in the top right of Figure 1.7, has resistance peaks occurring between 35 and 56 mV. The oxygen evolution Tafel slope used to generate these plots was 80 mV per decade, however 90 mV per decade has also been commonly stated<sup>ii iii</sup>. When the same corrosion current levels used in Figure 1.7 are added to an oxygen evolution slope of 90 mV per decade, the polarisation range associated with the peak equivalent resistance is shifted slightly, and is seen to be 39 - 63 mV. While this range appears very similar to the general range accepted by battery chemists to have minimum corrosion, no association verification has been undertaken. Any attempt to verify a correlation between the polarisation at which the peak in equivalent resistance occurs, and the polarisation producing minimum corrosion, would require significant electrochemical testing which is beyond the scope of this thesis. At this stage, the occurrence and similarities of this phenomenon must be considered purely coincidental. However, the similarities have been noted, and the influences producing the peak in equivalent resistance, and its location, have been explained.

No verification or proof has been undertaken to correlate the mathematical phenomenon of the peak equivalent resistance point with the minimum grid corrosion point. However, the often debated point or range of positive polarisations associated with minimum grid corrosion appears almost identical to the values obtained with a little mathematical manipulation of commonly found experimental data. This may warrant further experimental investigation and analysis. If a correlation between the mathematical peak in equivalent resistance and the corrosion minimum were experimentally proven, a chemistry free method of assessing the optimal positive polarisation for maximum life would be facilitated.

## **1.1.2 Energy Storage Capacitors, Bulk and Overcharge**

Section 1.1.1 described the model components required to reproduce the steady state overcharge characteristics of a VRLA cell. This section will describe the energy storage elements required to replicate the transient response of a VRLA cell as it moves from one steady state operating point to another. As some form of energy storage is required to slow the transition from one steady state operating point to the next, and due to the linear voltage decay produced when a constant current is drawn from a cell, capacitors are the obvious choice of model component. The model in Figure

1.1 employs a single variable capacitor for each electrode. Effectively, each of these capacitors has two values, one value for the bulk energy storage mechanism associated with the main charge-discharge reaction, and a second value associated with the polarisation transient response, which is significantly smaller.

The size of the total (positive plus negative) bulk storage capacitance is calculated from the voltage difference between the fully charged rest voltage and the discharged rest voltage, the discharge current, and the discharge time ( $C = i \cdot dt / dV$ ). Assuming that the fully charged and discharged rest voltages are 2.14 and 1.9 V, the equivalent capacitance required to represent the bulk storage is approximately 15,000 farads/Ah. Alone, this capacitor representation will produce an uncharacteristic linear voltage decay when a constant current discharge is applied. While this is significantly different to a typical constant current discharge curve, the model is targeted at the overcharge region of VRLA battery operation, and only a basic representation of the bulk storage is required. However, the discharge profile is significantly improved if the variation in the electrolyte resistance is modelled during the discharge, as will be shown in Section 1.1.4. Furthermore, as only a single capacitor is used to model the bulk storage of each electrode, the reduction in apparent available capacity with increased discharge rate is not modelled. Similarly, the bulk recharge characteristics are not accurately modelled. By applying a current-limited constant voltage recharge, it is expected that the current limit will be exercised until the cell voltage has risen to the charger voltage, and that this voltage will then be maintained as the charge current exponentially decays to the float value. As the bulk storage of each electrode is modelled by a single capacitor, when the float voltage is reached, the current drops directly to that required for float charge. If improved modelling of the bulk discharge and recharge characteristics is required, a distributed capacitor-resistor ladder type circuit may be necessary. This may be optimised to replicate the apparent reduction in available capacity seen in high rate discharges, and also to provide the exponential decay in recharge current when recharging with constant voltage. A distributed capacitor-resistor ladder type circuit should attempt to replicate the mass transport and kinetic limitations within a cell. However, as the developed model is intended for float charge analysis, the basic single capacitor representation of bulk storage at each electrode is sufficient, and requires minimal calibration.

The total capacitance used to model the main charge-discharge reactions must be distributed between the two electrodes. The software `vrla_part_size.m`, used to calculate the component

values for the simulation model, contains a parameter 'pos\_bulk\_percent' to allow the total bulk capacitance to be split as desired between the positive and negative electrodes. This allows each electrode's voltage-change ratio and the voltage supported on each electrode to be defined. For example, if the 'pos\_bulk\_percent' were set to 60, the positive electrode would provide 60% of the cell's voltage, and 60% of the change in the terminal voltage during discharge would be attributed to the positive electrode. As series connection decreases the total capacitance, the distribution of the total bulk-storage capacitor must be such that each electrode produces the desired voltage-change during discharge, and that the series combination of the two capacitors still equals the required total. While the theory of sizing the capacitance of each electrode to produce a desired voltage-change during discharge is valid, the dominant reason for the characteristic shape of the discharge profile is due to an increasing electrolyte resistance. Voltage drops associated with electrolyte resistance overshadow the differences in each electrode's voltage decay. At high discharge rates, the apparent distribution of discharge voltage-change is more heavily influenced by the simulated location of the reference electrode (division of acid resistance) than the actual voltage-change on each electrode. The component value selection software also calculates a voltage offset (to be added to the model's centre, or reference, point). This offset voltage is the difference between the model's centre point voltage (centre of acid resistance) and the voltage that would be produced when a  $\text{Hg/Hg}_2\text{SO}_4/\text{K}_2\text{SO}_4$  reference electrode is used on a cell in the same charge state. The offset voltage effectively normalises the voltage obtained by the simulated reference electrode as the 'pos\_bulk\_percent' is altered. The simulated reference-electrode does not reveal the actual voltage supported on each electrode's capacitor. A 'pos\_bulk\_percent' value of 75% was found to be the most suitable and has been used for all simulations.

Having calculated the total required bulk storage capacitance and an appropriate distribution for each electrode, the capacitors required to produce the overcharge transient response must also be calculated. Due to variance between batteries, no precise method of determining the overcharge capacitor size for each electrode has been established. However, it has been found that 0.3% of the total bulk storage capacitance is suitable as an initial value for the overcharge capacitance of the positive electrode, and that 0.005% is suitable for the overcharge capacitance associated with the negative. Having calculated these initial values, simulation results can be compared with experimental data, and the overcharge capacitance values fine-tuned so that simulation results replicate experimental data.

Figure 1.8 shows the transition between the bulk storage capacitance and the overcharge capacitance of each electrode. It can be seen that as the electrode voltage rises above the zener voltage, there is a rapid decrease in the capacitance to the overcharge value. To provide a smooth change between the two capacitance values, a transition region has been defined. Below the zener voltage for each electrode, the capacitor has the value calculated for the bulk storage of that electrode. Inside the transition region, the capacitance is a function of the electrode voltage as shown by Equation 3), while above the transition region, the capacitance has the value calculated for overcharge. Suitable transition regions have been found to be 40 mV for the negative electrode, and 10 mV for the positive.

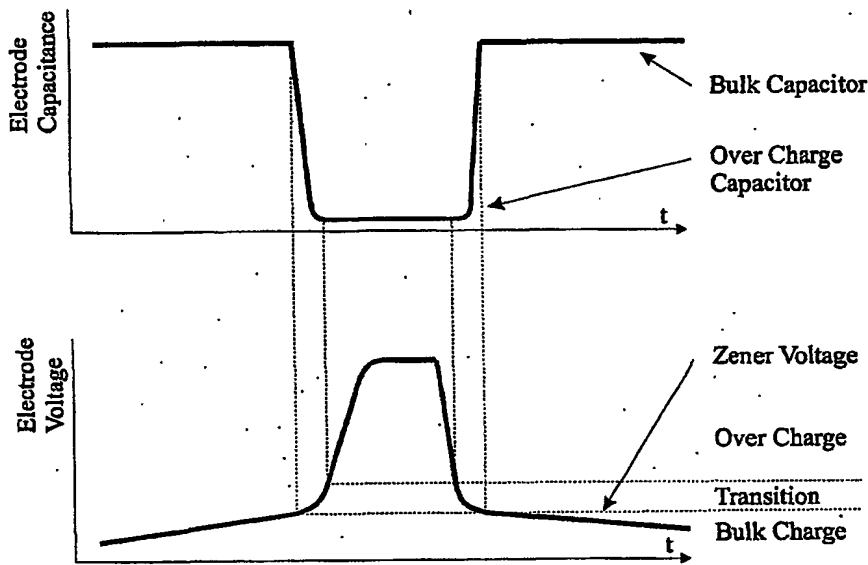


Figure 1.8 Transition of Bulk Storage and Overcharge Capacitance Values

$$C_{trans} = C_{ochg} - 1 + (C_{bulk} - C_{ochg} + 1) \left( 1 - \left( \frac{V_{cap} - V_{zen}}{V_{trans}} \right) \right)^s \quad 3)$$

where,  $C_{trans}$  = Capacitance during transition  
 $C_{ochg}$  = Overcharge Capacitor Value

Value

$C_{bulk}$  = Bulk-Charge Capacitor

$V_{cap}$  = Capacitor Voltage

$V_{zen}$  = Zener Voltage

$V_{trans}$  = Transition Voltage-Range

$S$  = Shaping Term (5 was used)

### 1.1.3 Zener Diodes

The zener diodes in the model are ideal, as when the capacitor voltage is below the zener voltage no reverse current flows through the diode. When the capacitor voltage is above the zener voltage, the current through the diode is determined by the value of the non-linear overcharge resistor, and the voltage across the same resistor. The voltage at which the zener diode begins to conduct is determined by the relative sizing of the bulk storage capacitors for each electrode. This is determined through the 'pos\_bulk\_percent' variable in the component value selection software `vrla_part_size.m` previously described in section 1.1.2.

### 1.1.4 Acid Resistance

As the electrolyte specific gravity, and hence resistance, does not change considerably in the float charge region of VRLA battery operation, a fixed value of acid resistance is sufficient for float modelling. However, by attempting to provide a more realistic voltage profile during the bulk discharge, the effects of the change in electrolyte resistance during discharge have been modelled. While the model of acid resistance effectively changes the overall resistance, it is still a single element model, and does not attempt to model time dependant quantities such as mass transport, electrolyte gradients, or kinetic properties.

The variation in electrolyte resistance is largely modelled on the long-standing guideline that the specific gravity of an open circuit cell is the voltage of the cell minus 0.85. As the sum of the voltage on the positive and negative electrodes' bulk-storage capacitors is equivalent to the open circuit voltage, this may be used to determine the specific gravity of the simulated electrolyte. A function is then used to calculate the specific conductance based on specific gravity. This specific conductance is then converted to resistance, and scaled so that the specified fully charged acid resistance is produced at the point at which the cell is fully charged and overcharge begins. As the

cell model enters the overcharge region, the electrolyte resistance is held constant at the value specified for the fully charged state.

Equation 4) shows the function used to calculate the specific conductance of the electrolyte based on the calculated specific gravity. Figure 1.9 shows a plot of the function in Equation 4), along with some values of specific conductance at 20°C found in the literature<sup>iv</sup>. It can be seen that above a specific gravity of 1.3, the function has some deviation from the literature values, however the specific gravity of the electrolyte used in VRLA cells is typically less than 1.3.

$$SC = SC_{PK} \times \left( \frac{|SG - C_{PKSG}|^{Shape}}{-1 \times |1 - C_{PKSG}|^{Shape} + 1} \right)$$

4)

where:  $SC$  = Specific Conductance

$SC_{PK}$  = Value of Conductance Peak ~0.76

$SG$  = Specific gravity

$C_{PKSG}$  =  $SG$  at the Conductance Peak ~1.235

$Shape$  = Curve Fitting Variable ~ 2.15

The required value of the fully charged electrolyte resistance must be determined from experience or battery manufacturers' data. However, as this parameter has very little influence on float analysis, a default value of 1 milli-ohm may be used. Generally speaking, the electrolyte resistance will be inversely proportional to cell capacity.



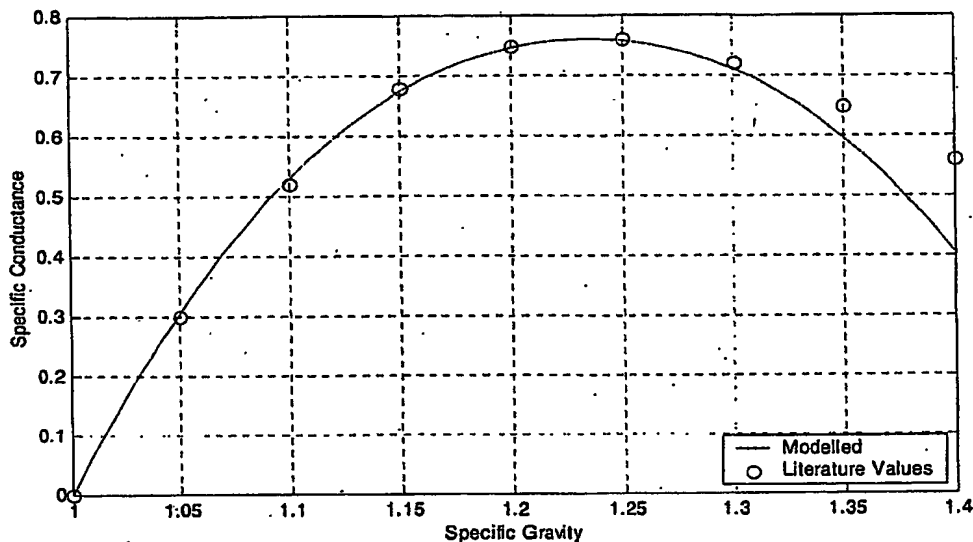


Figure 1.9 Electrolyte Specific Conductance as a Function of Specific Gravity

### 1.1.5 Metallic Resistance

Similar to the electrolyte (acid) resistance, the metallic resistance has very little influence on the float characteristics of a cell. However, for completeness, a single lumped-resistor simulating the effects of the current conducting path (grid) of each electrode has been included in the model. Again, no method of determining the value of the metallic resistors has been investigated, and default values of 10 micro-ohms have been used for all simulations. The sum of the acid resistance and the two metallic resistors should equal the internal resistance of the cell.

## 2 Model Limitations and Boundaries

The model described previously in this section was developed to replicate both the steady state and transient responses of a cell's positive and negative electrodes while on float charge. When the responses of each electrode are combined, the overall terminal response of a cell is reproduced. For a given float voltage, the model will draw the same float current as the cell it was modelled on, and for a given float current, the model will produce the same terminal voltage. This is true not

only for the steady state levels, but also the transient response, as the model is moved from one steady state operating point to another. As the model was developed for the analysis of a cell's operational state, it is not based on cell chemistry, or intended to directly explain this. However, it may be possible for certain features of the model to be interpreted from a chemistry perspective.

While the model was developed to replicate both the steady state and transient responses, only the most significant transient features overall have been modelled. Small features, such as the Coup de Fouet-like voltage overshoot and have not been modelled for either electrode. These overshoot and recoveries are seen as the electrodes enter the bulk charge region after spending time in the overcharge float region. However, as these features typically have small magnitudes (5 - 10 mV), and appear to lack magnitude and duration consistency, no attempts have been made to model these features.

As the model targets the float charge phase of VRLA battery life, only a very basic implementation of the main charge-discharge reaction has been modelled. The voltage change at the modelled cell terminals for a full discharge will be similar to that for a full discharge of a cell at the rate specified with the cell's nominal capacity. As implemented, the model will deliver the same (rated) capacity, regardless of the discharge rate. Cell kinetics limits the transport of the reacting species to and from the reaction site, and is largely responsible for the reduction in available capacity as the discharge rate is increased. As the model was not intended for analysis of the bulk charge and discharge regions of operation, no attempt has been made to replicate kinetic limitations within the bulk energy storage in order to reduce calibration requirements. For similar reasons, the model does not reproduce the exponential current decay seen when a cell is recharged with a voltage limit. While the model will reproduce the response of a cell at any temperature provided appropriate calibration data is supplied, the model will not replicate changes for a single set of cell calibration data in these operating characteristics due to temperature variation.

By modelling both electrodes within a cell separately, the terminal response of the cell may be decomposed into the response produced by each electrode without the aid of an additional reference electrode. While this would imply that a well-calibrated model is required, the electrodes' transient responses have been found to be sufficiently different that the model (and associated calibration) is not necessary for certain analyses, such as polarisation distribution estimation.

**THIS PAGE BLANK (USPTO)**

### 3 Applications

In this thesis an analysis of the float charge operation of VRLA cells has been undertaken. Two goals for float charge have been identified: 1) Ensuring the battery remains fully charged, and 2) Maximising the life of the battery. Through appropriate distribution of the polarisation applied to the cell by the float charge, both of the identified goals of float charge may be realised simultaneously. However, the cell's design and construction largely determine the manner in which this applied polarisation is distributed within the cell. To a much lesser extent, the total polarisation applied to a cell may be controlled in an attempt to optimise the level of polarisation on individual electrodes within the cell.

Through modelling the steady state and transient characteristics of each electrode within a cell, a test and analysis technique has been developed that estimates the polarisation distribution within a float-charging VRLA cell. While the outcome of this test produces similar information to that obtained through reference electrode testing, the test does not use any form of reference electrode, and may be applied to any standard 2 V VRLA cell without any modification to the cell.

It is understood that many 'long life' VRLA cells suffer from low or no polarisation on the negative electrode. This mode of operation produces several mechanisms that impact on a cell's life expectancy. If the float voltage is not appropriately adjusted, the low negative polarisation will produce increased positive polarisation, thus raising the level of life-limiting positive grid corrosion, and also the rate of overcharge gas production. If gas production is excessive, gas venting and premature failure through dryout can result. Low or non-existent negative electrode polarisation may also result in a gradual discharge of the electrode to the point where the available capacity of the cell does not meet the load requirements, forcing replacement of the cell.

The problems that lead to the premature failure of some VRLA cells have been described in this work, and a simple field useable test and analysis procedure for identifying these problems and measuring the success of the applied float charge has been developed. As this work has focused on the identification of these float charge problems, and the development of an analysis procedure suitable for widespread field use, the strategies or techniques that may be used to attempt to correct problem cells have not been thoroughly investigated. Section 3.1.3 suggests future work that could be undertaken in this control area now that the float assessment tools have been developed.

While the test and analysis procedure was primarily developed for the early detection of float charge problems so that corrective action might be taken before cell damage becomes apparent, there may be many other uses for the developed model and polarisation estimation technique. Section 3.1.1 suggests possible uses of the developed float charge model, along with future work and improvements that may be made to the model. Section 3.1.2 describes some alternative applications or uses of the developed test procedure that estimates the distribution of polarisation within a cell.

### 3.1.1 Model Uses

The developed float charge model may have many alternative uses besides the intended assessment of cells on float charge in the field. Some of these uses may include provision of simulations for product development and testing, or tracking variations in a cell throughout its life by detailing variations in component values within the developed model. The latter suggestion may provide a timely indication that the end of battery life is imminent, allowing replacement batteries to be purchased prior to the battery failure occurring.

Due to the low voltage of a single VRLA cell, a number of cells are normally connected in series to form a 'string' in order to achieve useable voltages. As the string length is increased, the equalisation or uniformity of cell voltages tends to be reduced. To equal the 400 – 600 V DC provided by some UPS batteries, some two to three hundred 2 V cells must be series connected. The developed float charge model may also be serially stacked to simulate the operation of such long strings, however a slight spread will need to be specified for parameters such as float voltage, current, and polarisation. This spread in component values may be defined for best or worst case, or a random spread may be simulated within a specified window. With the modelling of a string of slightly different cells, battery-monitoring algorithms, string level optimisation, control techniques, and cell level equalisation methods and techniques may be simulated, assessed, and optimised.

If sufficient information is gathered during testing or general battery the model may be accurately calibrated for each cell. Over time, the unchanged model will highlight variations in the operational characteristics of the cell, as these change. Re-calibration of the model will highlight the components of the model affected by the changes in the cell. Depending on the model

components that have altered, the cause of the change may be determined, and possibly linked to age, operation, or cell faults.

However, as the developed model targets the float region of VRLA battery operation, in its present configuration some of the traditional failure modes, such as grid corrosion, may not be appropriately modelled. Further work is necessary to improve the model's representation of the bulk charge and discharge regions of operation if a complete assessment is required. The traditional (designed) cell failure mode is grid corrosion, which causes an increase in the internal resistance of the cell, and eventually limits the current that can be supplied by the cell for a given voltage drop. Internal resistance problems are best highlighted through high rate charge or discharge tests, as these high rate tests tend to be used to indicate capacity related state of health or remaining life. The developed test assesses the float operation of cells. The accuracy of this assessment improves as the discharge rate is reduced. As the best results are produced from open circuit decay, internal resistance does not have a large influence on the developed test. The developed model essentially assesses the SOC while the cell is float charged. While it is understood that the float voltage variation between cells in the same string may be significant when the cells are new, this variation converges to a low value for the majority of the cell's useful life, and then diverges towards the end of life. Further work is required to determine whether the developed float charge model may be used to assess the changes in float characteristics as cells age, and to establish whether this may then be used to indicate imminent cell failure.

### **3.1.2 Test Procedure Uses**

The developed polarisation estimation test may have many applications besides the intended use of assessing cells in field service. The conventional method of assessing polarisation distribution in a laboratory involves the use of a reference electrode, however as a VRLA cell operates as a sealed unit, the addition of a reference electrode to a cell always has the potential to modify the cell's characteristics. It was seen in the first series of tests, using the ESPACE cell, that large variances in cell characteristics were produced through inconsistencies in the negative electrode Tafel line (intercept point). Atmospheric oxygen entering the cell through leaks in the case is said to have a depolarising effect on the negative electrode. Puncturing the cell's case to add a reference electrode must therefore increase the possibility of producing such leaks. As the developed polarisation assessment technique does not require any modification to the cell, the chances of altering the cell's characteristics must be reduced. The developed test may replace or supplement

conventional laboratory reference electrode testing used during the development and design verification of new products. The polarisation estimation test may be extremely useful during accelerated life testing undertaken at elevated temperatures, where the use and maintenance of reference electrodes is difficult.

The developed polarisation estimation test procedure may also be used to verify the operation of cells after their manufacture, before they leave the factory. As newly manufactured cells are likely to have excessively wet separators, the paths through the separator required for oxygen recombination may not be fully developed. A new cell may therefore operate as a flooded cell until sufficient gas has vented, and the separator has dried to the point where recombination gas paths are developed. As flooded cells are expected to have well polarised negative electrodes, the absence of this may highlight electrolyte-filling problems, or possibly case sealing problems. The voltage decay profiles measured on cell terminals for open circuit or low rate discharges may be used to indicate product consistency.

### **3.1.3 Float Charge Optimisation**

Without knowledge of the polarisation distribution within a cell, any attempt to optimise the float charge must be based on historical data from other cells of similar type, generic empirical rules of thumb, or recommendations from laboratory based testing of the same cell type. As no simple or practical method of assessing the polarisation of standard cells was available, individual cell based float charge optimisation has not been possible.

In this thesis a model of the float charge region of operation of a VRLA cell has been presented, and a test and analysis technique has been developed to provide an estimate of the polarisation distribution within any standard 2 V VRLA cell. While this model was essential for the development and verification of the test and analysis technique, a calibrated model is not essential for analysis of a cell's polarisation. The developed testing technique requires only the cell's polarisation decay profile for polarisation estimation.

As the majority of this work has focused on developing the tools necessary to obtain polarisation estimations, little work has been undertaken on optimisation techniques and strategies to ensure both float charge goals are achieved. For a well designed cell that displays consistent textbook

Tafel characteristics, the optimisation should be simple and uncomplicated. However with cells identified to be suffering from electrode polarisation problems (either positive or negative), the optimisation may be more complicated. The two cells extensively tested in this thesis were both shown to have poor electrode polarisation distributions. When the float voltage was varied on both of these cells, unexpected redistribution of the applied polarisation resulted.

It is believed that a large number of VRLA cells in field service suffer from electrode polarisation problems, the most predominant of which is negative electrode discharge. Further work is required to determine appropriate control strategies to that ensure the cell is maintained in a fully charged state, and that maximum life for the defective cell is realised. For example, two courses of action may be available should a cell be proven to be suffering from a gradual discharge of the negative electrode. It must be determined whether it is more beneficial to: a) raise the float voltage in an attempt to polarise the negative electrode, at the expense of increased positive grid corrosion and possible dryout resulting from gas venting, or b) reduce the float voltage, giving the positive electrode optimal polarisation for minimal grid corrosion, and perform regular boost charges to ensure that the negative electrode is periodically fully charged.

When cells are charged in a series string, a spread in the terminal voltages of individual cells is often seen. The developed polarisation estimation technique may be used to assess the benefits or disadvantages of various cell voltage equalisation schemes. The advantages of natural voltage (no equalisation), uniform voltage equalisation, and optimal voltage for each cell using individual positive polarisation values may be compared to determine the scheme that best fulfils the float charge goals for the entire string.

Temperature compensation is a common technique that is used when cells are operated at temperatures either higher or lower than the designed operating point. While temperature compensation may reduce overcharge gas production levels and the possibility of thermal runaway, it does not maintain an optimal polarisation for minimum grid corrosion. Because the developed polarisation estimation assessment technique is unaffected by temperature, the polarisation at the compensated float voltage may be assessed following initial application of the recommended temperature compensation. This will determine whether the float voltage is appropriate, and whether the goals of float charge have been achieved.



Conventionally, a specific single float charge voltage is recommended for a given cell type, regardless of its age. The developed polarisation assessment technique will allow an optimal float voltage to be maintained throughout the life of the cell. This may compensate for cell characteristic variations due to age, or operational history. Further work would be required to assess the advantages or disadvantages of such an optimisation system.

A simple tool has been developed to provide an assessment of the polarisation distribution within any standard 2 V VRLA cell. With the information provided by this test, many float charge optimisation schemes may be assessed and compared. The developed tool will identify cells with float charge problems before permanent damage is done, and also provides a measure of the success of the float charge, allowing the effectiveness of any correction or optimisation techniques to be assessed. As a tool is now available to assess the operation of VRLA cells on long term float charge in field service, float charge problems may be identified promptly. This allows corrective action to be taken in the early stages, before the problems escalate to levels where unrecoverable damage is sustained by the cell.

---

<sup>i</sup> D. Berndt, *Maintenance-Free Batteries Lead-Acid, Nickel/Cadmium, Nickel/Metal Hydride A Handbook of Battery Technology Second Edition*, Research Studies Press Ltd. Taunton, Somerset, England, John Wiley & Sons Inc. New York, Chichester, Toronto Brisbane Singapore, 1997. pp 161.

<sup>ii</sup> D. Berndt, U. Teutsch, *Float Charging of Valve-Regulated Lead-Acid Batteries: A Balancing Act Between Secondary Reactions*, Journal of the Electrochemical Society., Volume 143, No 3, March 1996.

<sup>iii</sup> H. Bode, Translated by R. J. Brodd & K. V. Kordesch, *Lead-Acid Batteries*, The Electrochemical Society Series, Wiley-Interscience (a division of John Wiley & Sons) 605 Third Avenue, New York, N.Y. 10016, New York. London. Toronto. Pp 315.

<sup>iv</sup> D. Berndt, *Maintenance-Free Batteries Lead-Acid, Nickel/Cadmium, Nickel/Metal Hydride A Handbook of Battery Technology Second Edition*, Research Studies Press Ltd. Taunton, Somerset, England, John Wiley & Sons Inc. New York, Chichester, Toronto Brisbane Singapore, 1997. Fig 4.20, pp 144.

## TESTS

### 1.1.1 Transient Test

The initial testing identified the use of differences in the transient response of the positive and negative electrodes' polarization as a means of estimating the polarization of each electrode. To further investigate the possibility of using transient response as an analysis tool, and to examine how variations in operating conditions affect the transient response, the tests detailed in Sections 1.1.1.1 and 1.1.1.2 were performed. The analysis of the testing has been undertaken to isolate the effects of applied float voltage and discharge rate. All analysis in this section assumes the cell temperature to remain between 22 and 23 °C.

#### 1.1.1.1 Constant Voltage, Variable Discharge Rate

Figure 1 shows the effects of discharging a cell that has been float charged at a voltage that is too low. It is hypothesized that when a cell is not fully charged, the dual-slope rapid decay associated with the discharging of the polarization capacitance would not be present. Instead, the response of the cell is expected to be a simple, steady decay associated with the discharge of the main storage reaction.

To be sure that the cell under test was not fully charged, it was first discharged to approximately 80% Soc (this should settle to an open circuit voltage of approximately 2.09 V) and then charged with a supply set to 2.1 V. As the fully charged open circuit voltage for this cell is approximately 2.14 V, a charge voltage of 2.1 V should result in the cell being 'float charged' at only 85% SOC. The cell was charged at 2.1 V until steady state (no change in charge current) was achieved before the discharge testing plotted in Figure 1 was initiated. The terminal voltage was maintained in a tight group at approximately 2.1 V prior to the discharge. With the exception of the 10 A discharge, there appears to be a drift of the electrode potentials with each successive test. It is seen that the potential of the positive electrode increases with each test. The reason for the 10 A discharge not following the trend is due to the testing order. As virtually no decay was seen in the first (open circuit) test, the 10 A test was brought forward to the second test performed so that it could be determined whether a measurable response would be obtained. Having verified a

measurable response, the remainder of the testing at 2.1 V was performed in the planned order (10 mA, 100 mA, and 1 A). While care was taken to visually ensure the achievement of steady state conditions before initiating the next test, time limitations resulted in finite settling times. Reasoning for the drift in electrode potential below open circuit is not essential to the outcomes of this research, and therefore the cause has not been investigated. However, it is speculated that the drift may be related either to the finite settling time, or to differences between discharge and recharge efficiency of each electrode at this operating point.

As expected, it can be seen in Figure 1 that at low currents (open circuit to 100 mA) there is virtually no change in the cell's terminal voltage when the charge is removed and the discharge commenced. As the discharge current is increased, an increased rate of voltage decay for the cell and each electrode can be seen. This is a combination of increased voltage drops due to resistive components, and an increased rate of cell discharge. The response of the negative electrode to higher discharge rates shows an initial drop followed by a constant voltage, suggesting a large capacitor and series resistor may be used as a model. When compared to the negative, the response of the positive electrode at high rates has a significantly slower and larger initial drop, followed by a slow continuous decrease in electrode voltage. This suggests that a similar series resistor-capacitor model would require a slightly smaller capacitor and a larger resistor. The modeled positive resistance may also require a small capacitor in parallel with the resistor to give the slower response of the initial drop.

It can be seen in Figure 1 that almost no change in the terminal voltage occurs with discharge rates lower than 1 A. This is desirable, and in keeping with the proposed model. If the bulk charge capacitors are orders of magnitude bigger than the overcharge capacitors, it is expected that when there is no polarization, the change in terminal voltage from low rate discharges will be very slow. Test currents of a magnitude similar to or lower than the float current are preferred, as resistive drops are seen to have very little influence on the response voltage. No terminal voltage response is seen when no polarization exists.

Figure 2 shows the response of various discharge rates for a cell that has been float charged at approximately 2.2 V. The fully charged open circuit voltage for this cell is 2.140 V at 200C. When measured against a Standard Hydrogen Electrode (SHE) the positive electrode has a fully charged open circuit potential of 1.738 V, and the negative electrode has a potential of 0.402 V.

During the series of tests conducted at a float voltage of 2.2 V, it was noted that the potentials of each electrode prior to the discharge did not correspond to the first Tafel plot. It can be seen in Figure 2 that prior to the discharge, the positive electrode has a potential of approximately 1.76 V with respect to (wrt) SHE, and the negative electrode's potential is -0.438 V wrt SHE. A Tafel test suggests that at this test voltage, the positive electrode should have a potential of approximately 1.8 V, and the negative 0.4 V wrt SHE. As a significant amount of negative electrode polarization is seen prior to the discharge in Figure 2, it was suspected that the battery characteristics might have changed as a result of testing. At the end of this series of tests another Tafel plot was conducted. While this plot does show a small peak of approximately -425 mV in the negative electrode potential at a cell voltage of 2.2 V, there is still a discrepancy of 15 mV between the Tafel and transient tests. It is suspected that this may be related to settling time limitations in the Tafel plots. Electrode potential plots in Figure 2 typically took three to four days to settle to steady state (prior to the discharge), however the current used for steady state detection in another test stabilized much faster.

It can be seen in Figure 2 that the response of the positive and negative electrodes is as expected. At the low discharge rates (open circuit to 100 mA) the negative electrode is seen to decay to the fully charged open circuit potential, while there is very little response from the positive electrode. At the 1 A and 10 A discharge rates, a decrease in the positive electrode potential is seen, however when compared to the near instantaneous drop of the negative at these rates, the transient response of the positive electrode is significantly slower. Also evident at the higher discharge rates is a small 10-20 mV recovery on the negative electrode following the initial voltage. This recovery appears to coincide with the point in time at which the positive electrode polarization is discharged.

The negative electrode's fully charged open circuit voltage for the cell tested in Figure 2 is approximately -400 mV. As the discharge rate is increased, the negative electrode is seen to decay to lower voltages. It is believed that the potential differences are due to resistive effects. At discharge rates of a similar magnitude to the float current, the influence of these resistive volt-drops is negligible. Again, similar to the plots shown in Figure 1, it is evident in Figure 2 that each successive test has a small drift in electrode potential prior to the discharge. This drift increases the potential of the positive electrode at the expense of the negative.

Figure 3 shows the previously tested cell discharged from a float voltage of approximately 2.3 V. As the 2.3 V series of tests was the first to be conducted, it is appropriate to compare these tests to the first Tafel plot. The Tafel plot shows that at a cell voltage of approximately 2.3 V the negative electrode is just beginning to polarize, and has a potential of approximately -410 mV. This correlates well with the open circuit plot in Figure 3. Similarly, the Tafel plot shows a positive electrode potential of approximately 1.89 V, which again correlates well with the positive electrode's potential seen prior to the open circuit plot (Figure 3). However, as the testing progresses, a shift in the electrode potentials can be seen prior to the discharge. The change in potential of the negative electrode is seen to increase as opposed to the positive increasing in the previous two plots (Figure 1 and Figure 2). While the reason for this change is unknown, it may be related to the repeated shallow discharging during testing. The trend of increasing negative electrode potential with testing is supported by later Tafel plots.

Prior to the discharge testing, the difference between the float voltages in Figure 1 and Figure 2 is approximately 100 mV. With a fully charged open circuit voltage of approximately 2.14 V, the 2.2 V tests have a total polarization of 60 mV, while the 2.3 V tests have a total polarization of 160 mV. For float charge optimization, it is important to know how this total polarization is distributed between the positive and negative electrodes at the operated float voltage. It can be seen that as the float voltage is increased, there is an increase in the potential of the positive electrode, and a decrease in the potential of the negative. Comparison at a similar discharge rate, for example 100 mA, shows that the potential of the positive electrode increases by 123 mV, from 1.760 V at a cell float voltage of 2.2 V, to 1.883 V at a float voltage of 2.3 V. Similarly, it can be seen that the potential difference (wrt SHE) of the negative electrode has decreased by 24 mV, from -438 mV at a float voltage of 2.2 V, to -414 mV at a float voltage of 2.3 V. As the fully charged open circuit potential of the negative electrode is approximately -400 mV, there is about 14 mV of negative polarization at a cell float voltage of 2.3 V, and 38 mV at a float voltage of 2.2 V. The fully charged open circuit potential of the positive electrode is approximately 1.74 V. At a float voltage of 2.2 V the positive electrode has approximately 20 mV of polarization, while at a float voltage of 2.3 V this is 143 mV. As the optimal positive electrode polarization for minimal grid corrosion is accepted

to be between 40 - 70 mV, a float voltage should be found between these two operating conditions to produce the desired result.

On comparison of the cell voltage discharge profiles in Figure 2 and Figure 3, it can be seen that although the discharge rates are similar, the rate of voltage decay is faster in Figure 3. As the initial response in both plots is almost entirely from the negative, it would be expected that with more negative polarization, the rate of decay in Figure 2 would be faster. It is, however, seen to be slower. Dependant on the discharge rate, the decay of the negative electrode's polarization takes up to take up to ten minutes in Figure 2, while in Figure 3 this is seen to be less than one minute at all discharge rates. While the reason for this feature is related to the cell's chemistry and is not subject to investigation in this research, it is speculated that the increased rate of decay in Figure 3 may be due to a greater depolarizing effect from oxygen recombination. As Figure 3 has significantly more polarization, it is expected that there will be more production and corresponding recombination of overcharge gas. As oxygen recombination is said to have a depolarizing (slight discharging) effect on the negative electrode, the increased positive polarization may explain the increased rate of negative polarization voltage decay in Figure 3. While small differences in the rate of the negative electrode polarization decay have been noted, these are not significant when compared to the rate of polarization decay of the positive electrode. Furthermore, these slight variations do not affect the ability to use the transient response to externally determine the polarization distribution within the cell.

Excluding the high rate (10 A) discharge, Figure 3 shows a rapid (less than one minute) decay of the negative electrode to within 10 mV of it's fully charged open circuit potential. An overshoot (settling period) and recovery is seen on the 10 A discharge, with the recovery appearing to coincide with the time at which the positive electrode reaches it's fully charged open circuit potential. While the overshoot and recovery is visible on the 10 A discharge, it is also present to a lesser extent on the lower rate discharges. However, as the magnitude of the overshoot appears to be proportional to the discharge rate, the overshoot is not obvious at low discharge rates, and the recovery occurs outside the plotted region. Over the period of this negative electrode decay there is less than 10 mV change in the potential of the positive electrode.

Figure 4 shows the cell and each electrode's responses to various discharge rates after being float charged at 2.35 V. In keeping with previous analysis, the

discharge response of the negative electrode is still significantly quicker than the positive. Less than one minute is required for the negative electrode's polarization to decay, and during this time there is virtually no change in the positive electrode's potential. It can again be seen that the negative electrode temporarily overshoots to a slightly lower potential than the fully charged open circuit value before a recovery is made. The magnitude of this overshoot is again dependent on discharge rate, with an overshoot of approximately 16mV for a 100 mA discharge rate. It is noted that the amount of overshoot has increased slightly from that evident in the series of tests conducted at a float voltage of 2.3 V. The electrode potentials prior to the discharge in Figure 4 are in reasonable agreement with other tests.

Assuming that the fully charged open circuit voltages of the positive and negative electrodes are 1.74 V and 0.4 V respectively, it can be seen that at a float voltage of 2.35 V there is about 160 mV of positive polarization, and 50 mV of negative polarization. With the prior knowledge that the fully charged open circuit terminal voltage is approximately 2.14 V, the 2.35 V float charge suggests that there is 210 mV of polarization. By simply measuring the initial terminal voltage drop at the beginning of a light discharge, it is possible to estimate that there were 60 - 70mV of negative polarization, and that the remaining polarization (140 - 150 mV) is associated with the positive electrode. While there is a slight 10 - 20 mV underestimate of the positive electrode's polarization, it is clear that the polarization is well outside the desirable 40 - 70 mV window. If polarization estimations were to take into account negative overshoot, tighter polarization estimations may be achieved.

#### 1.1.1.2 Constant Discharge Rate, Variable Float Voltage

Figure 5 through Figure 9 show the effects float voltage has on the polarization discharge response. In a given figure, all plots have the same discharge rate. Prior to the discharge the test cell had reached steady state at the indicated float voltage. In all plots the 2.1 V float charge is intentionally below the fully charged open circuit voltage, in order to differentiate the responses of a fully charged cell and a cell not fully charged due to a low float setting. As the 2.1 V float charge plots are not fully charged, polarization does not exist, and these should therefore not be used for comparison of transient polarization decay trends.

Figure 5 shows the open circuit decay when the float charge is removed. It can be seen that for the plots starting from 2.2, 2.3, and 2.35 V, the negative electrode eventually settles to an open circuit potential of approximately -400 mV after 24 hours. However, in the short term (10 - 20 minutes) up to 20 mV difference in the negative's potential is evident. This stems from a 10 mV overestimate caused by an overshoot in the trace with strong positive polarization, and a 10 mV underestimate from the trace with minimal positive polarization. Similarly, the negative electrode's polarization decays much faster in the plots demonstrating significant positive polarization.

If an initial drop in terminal voltage when the float charge is removed is used as an estimate of the negative electrode's polarization, the accuracy of this estimate is seen to be  $\pm 10$  mV. This drop should be obvious well within the first hour following the removal of the float charger. If no significant drop is seen and the cell voltage is above the fully charged open circuit voltage (often given in battery specification manual), it may be assumed that the cell is suffering from negative plate discharge. If the terminal voltage decays to the fully charged open circuit voltage within the first hour, it may be assumed that the cell is suffering from positive plate discharge.

The plots in Figure 6 show the effects that float voltage variations have on the voltage response of a 275 Ah (C20) cell when a 10 mA discharge is applied.

Excluding the plot beginning at 2.1 V, after approximately 20 hours the negative electrode potentials form a relatively tight group around -400 mV. After the same period there is slightly more separation in the potential of the positive electrode, ranging from 1.72- 1.738 mV. However the lower two traces, starting at float voltages of 2.3 and 2.35 V, do show a gradual Coup de Fouet-like voltage recovery past the plotted region. On a much shorter time scale, it can be seen that the negative electrode of the 2.2 V float charge takes approximately 13 minutes to decay to its fully charged open circuit potential. The negative electrodes of the plots starting at float voltages of 2.3 and 2.35 V show a significantly quicker decay of approximately one minute, and some overshoot. The maximum negative overshoot is seen to be 13 mV, associated with the plot starting from the highest (2.35 V) float charge. Again, it is speculated that the increased rate of negative polarization discharge and overshoot are due to the level of positive polarization.

For the higher float voltages it takes approximately 20 hours to discharge the positive polarization at the 10 mA rate. This is significantly longer than the period of



time (up to 15 minutes dependant on associated positive polarization) taken to discharge the negative polarization capacitance. With such a vast difference in discharge times it is a relatively simple task to associate the shape and characteristic of the terminal response to that of each electrode. Virtually no change in the potential of either electrode (or the combined terminal response) is seen when a 10 mA discharge is applied to a cell that is not fully charged. The plot with a 2.1 V float charge is estimated to have a SOC of approximately 85%, with no significant change in cell voltage even after 20 hours of 10 mA discharge.

The plot in Figure 7 is similar to the previous two plots, however in this plot the test cell is subject to a constant discharge current of 100 mA. Very similar trends are seen, however the time scale is reduced due to the increased discharge rate. It can be seen that the negative electrode still rapidly decays and slightly overshoots it's fully charged open circuit potential. The worst case of overshoot is approximately 15 mV, and is similar to that seen in the previous plot. The duration of the polarization decay of both electrodes has decreased with the increased discharge current. The shortest (worst case) positive polarization decay takes two to three hours, while the longest time taken for the negative polarization to decay is four to five minutes. Virtually no change in the positive electrode's potential is seen over this short negative polarization decay period. It is therefore obvious that separating the responses of each electrode is still possible.

As expected, the 1 A constant current discharge plots detailed in Figure 8 show significantly reduced polarization decay times. Dependant on the level of polarization at the start of the discharge, the positive electrode's polarization decay ranges from 30 - 45 minutes, and the negative electrode ranges from 18 - 30 seconds. At the 1 A discharge rate, the amount by which the negative electrode temporarily overshoots its open circuit potential is seen to increase. At this rate, overshoot is seen in all plots and has a magnitude ranging from 8 - 18 mV. Overshoot is visible in plots showing low amounts of positive polarization. The increased level of overshoot is suspected to be due to increased resistive-volt-drops associated with increased discharge current.

Due to the increased discharge rate, the overshoot recovery is more obvious, and reasonably well aligned with the end of the positive polarization decay. A very small response of less than 8 mV is seen in the cell that is not fully charged. This is also believed to be largely due to resistive effects and should not affect the analysis. Using the significant time differences, the terminal response may be separated into that of

each electrode, however the increased current causes resistive volt drops to cloud the measured response.

Figure 9 shows the discharge profiles from several float voltages for a cell that is discharged at a constant 10 A rate. As expected, the relatively high discharge rate reduces the time required for the polarization to decay, with the positive electrode taking three to six minutes, and the negative taking only three to nine seconds. The amount of negative electrode overshoot also increases at this discharge rate, ranging from 20 - 33 mV. However the recovery of the negative electrode still corresponds to the point at which the positive polarization has become discharged. The increased negative electrode overshoot is believed to be due to resistive volt-drop increases associated with the increased current. This effect is also seen in the plot of the cell that is not fully charged. The plot starting at 2.1 V shows a 30 mV decay after one minute. This is significantly more than the slope expected for the main discharge reaction at a 10 A discharge rate. When the high rate discharge profiles are compared to those of the lower rates (or open circuit), the exponential decays seen at low rates appear to become linear. Similar characteristics in electrode discharge profiles are present at both high and low rates, however the effect of resistive elements and associated voltage offsets make estimation of the electrode polarization and distribution more difficult at high discharge rates. There are significant time advantages when using a high rate discharge polarization estimation test, as the test may be performed in a matter of seconds, rather than tens of minutes as required for the open circuit decay.

#### 1.1.1.3 Transient Test Summary

Through the use of reference electrode testing, it has been shown that the polarization of both the positive and negative electrodes has a characteristic similar to that of a parallel resistor-capacitor combination. Although capacitors associated with polarization are very small, when compared to an equivalent capacitance for the main charge-discharge reaction, polarization capacitance is significant and may be used to analyze the float charge operation of a cell. It has also been shown that there is a significant difference in the capacitance associated with the polarization of the positive and negative electrodes. The differences between the capacitance of the positive polarization, negative polarization, and bulk charge storage may be exploited.

to determine the polarization of each electrode within a cell without the use of a reference electrode.

When a cell is discharged, both electrodes within the cell are subject to an identical current. Differences in the effective polarization-capacitance result in dissimilar discharge duration for each electrode. It has been shown that the duration of the positive electrode's polarization discharge is typically about 100 times longer than that of the negative. However, this has been seen to range from about 30 to 1400 times. Even at the lowest end of this range, when the negative electrode's polarization has become discharged, there is negligible change in the potential of the positive electrode.

With analysis of the polarization discharge profile, it is possible to determine the contribution each electrode makes to the total polarization. It has been shown that the initial fast transient is almost entirely due to the polarization decay of the negative electrode. The positive electrode is responsible for the remaining slower polarization decay to the fully charged open circuit voltage. If the voltage drop associated with the negative polarization decay is subtracted from the total polarization, the amount of positive polarization may be estimated without further discharging the cell, and more importantly, without significantly altering its state. The total polarization is a simple calculation of subtracting the settled fully charged open circuit voltage from the float voltage.

Significant reductions may be made to the required test duration by increasing the discharge current. At high discharge rates, the influence of resistive elements within the cell produces current dependent voltage offsets in the measured transient response. At discharge rates up to a similar magnitude to that of the normal float current (approximately 1000), the effects of these resistive elements are seen to be negligible. At a discharge rate of  $C/1000$ , the test duration should typically be less than ten minutes and require less than 0.02% of the cell's capacity to be discharged.

Under certain conditions the rapid response of the negative electrode is seen to overshoot its fully charged open circuit potential. This is normally followed with a slight recovery back to the open circuit potential as the positive electrode's polarization becomes discharged. While it may be possible to explain the reason of this overshoot and recovery through cell chemistry and reactions, this is beyond the scope of this investigation. It is speculated that as the amount of overshoot appears to increase with positive polarization, the overshoot is related to the depolarizing effect

oxygen recombination has on the negative electrode, because less oxygen is produced with lower positive polarization values. The discharge rate also appears to influence the magnitude of the overshoot, with the amount of overshoot being seen to increase with increased discharge rates. When using recommended float voltages and  
5 discharge rates less than C/1000, the amount of negative overshoot is typically seen to be less than 10 mV. Considering the window of optimal positive polarization is 30 mV wide (40 - 70 mV), a 10 mV offset in the estimate should not severely degrade the test result.

It has been shown that the discharge duration associated with the polarization  
10 of the positive and negative electrodes differs considerably. As the amount of capacitance associated with polarization is extremely small when compared to the total stored energy, very low discharge rates (or even natural open circuit decay) are required to properly view the profile. Low rate discharge testing also reduces the effects of resistance-based current dependent voltage offsets in the measured  
15 response. Analysis of the polarization discharge profile, between the float voltage and the stabilized open circuit voltage, allows the polarization voltage of each electrode to be assessed. Primarily, this may be used to ensure that both electrodes within a cell are fully charged. A secondary function of this is that the positive electrode's polarization may be used to determine the cell's most appropriate float voltage, thus  
20 minimizing positive grid corrosion. The hardware needed to perform the analysis requires only an extremely low rate discharge unit, and voltage measurement. This test may be automated and performed on any VRLA cell in field service that has access to the cell's terminals. Due to the low power requirements, both test hardware and installation costs should be minimal.

25

### **1.1.2 Temperature Testing**

All of the analysis and testing performed in the previous section was undertaken at a room temperature of approximately 22 °C. It is a commonly accepted guideline that for every 8 - 10 °C increase in battery temperature, the reaction rates  
30 within the battery are doubled. It is expected that the overall polarization decay may vary as the battery temperature is varied, however the response time ratios of the positive and negative should remain similar.

Figure 10 compares the steady state (Tafel) characteristic of a cell at temperatures of 25, 35, and 45 °C. In keeping with the above guideline, it can be seen that for a given float voltage, e.g. 2.25 V, the float current approximately doubles with each 10 °C increment in temperature. The drop in current at approximately 2.15 V indicates a slight reduction in the cell potential at which the negative electrode begins to polarize, however overall steady state characteristics remain reasonably consistent as the temperature is varied.

Taking into account the expected variations caused by temperature changes, a comparison of Figure 10 and other test show the plots in Figure 10 to be more consistent. After the final planned Tafel plot (Test 50), in an effort to improve test consistency, further tests were used to make improvements to the Tafel testing control code. Additional tests relate to the 45, 25, and 35 °C plots in Figure 10. These were performed under identical settling times and maximum slope values. The modifications to the test code included lengthening settling times, more stringent slope requirements, and the addition of an absolute value current slope detection condition. This was necessary as under certain conditions, the current drawn by the cell following a step increase in voltage does not always decay to the steady state value as expected.

Before the negative electrode begins to polarize, a step increase in cell voltage instantaneously increases the current drawn by the cell. This increased current gradually decays to the steady state value. However, when the negative electrode begins to polarize, the current characteristic changes. A step increase in cell voltage is accounted for almost entirely by polarization of the negative electrode, while there is only a small increase in the current drawn by the cell. As the cell stabilizes to the new float voltage, there is a redistribution of the polarization gained by the negative. The positive electrode gradually increases its polarization, with a corresponding decrease in the negative. As the polarization gained by the negative electrode partially redistributes and stabilizes to an increased polarization on the positive electrode, there is a slight increase in the current drawn by the cell at that float voltage. As an increasing current (+mA/Hr) is greater than the minimum negative slope (-xx mA/Hr) used to detect stable current, an increasing current would result in premature detection of current stabilization. In order to resolve this problem, the

detection criterion was changed to ensure the absolute value of current slope is less than the stable detection limit.

Although premature detection of a stable current will change the results significantly, the effects should not be noticed due to the two-stage steady state detection used. The first stage of steady state detection requires the current drawn by the cell to be stable, while the second ensures that the electrode potentials are stable. If both current and voltage measurements are stable, all voltage, current, and temperature Figure 10 shows how the steady state float characteristics of a cell change with temperature. It can be seen that as the temperature is increased, as expected the characteristic remains largely unchanged apart from an increase in current. Figure 11 shows an open circuit decay of a cell at 450°C. It can be seen that from the float voltage of approximately 2.29 V, there is a rapid and almost instantaneous decay of the negative electrode's polarization to its fully charged open circuit potential. The positive electrode is seen to take approximately four hours to decay to its fully charged open circuit potential. During the short period required for the negative electrode's polarization to discharge, there is virtually no change in the potential of the positive electrode. While the increased temperature has significantly reduced the time required for the polarization to discharge in comparison with the plots at 22 °C in Section 1.1.1, the large difference in discharge duration of each electrode is still present. Transient analysis of a cell's terminal voltage profile during a low rate (or open circuit) discharge is still able to resolve the response of each electrode within the cell, and determine their polarization. Cell temperature may alter the overall duration of the transient test, however, the relative response differences of each electrode still exist.

## TEST FIGURES

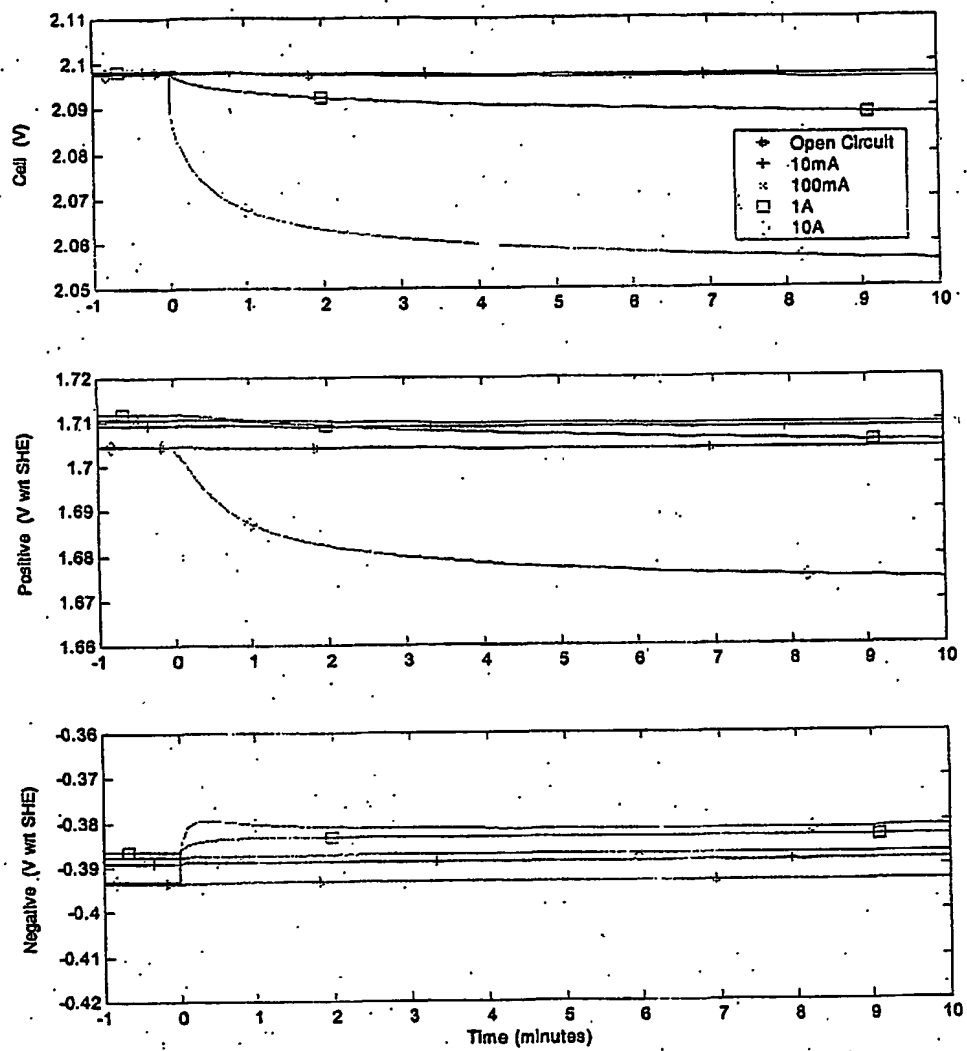
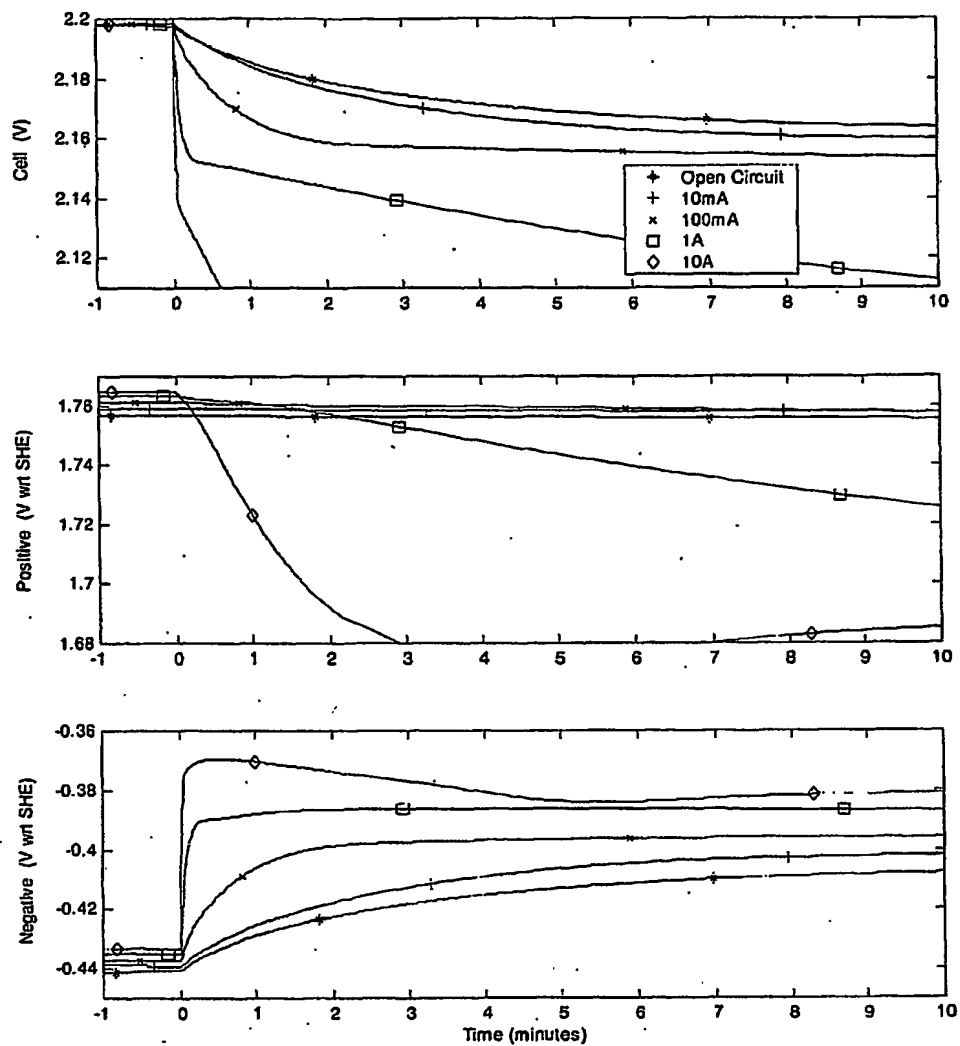
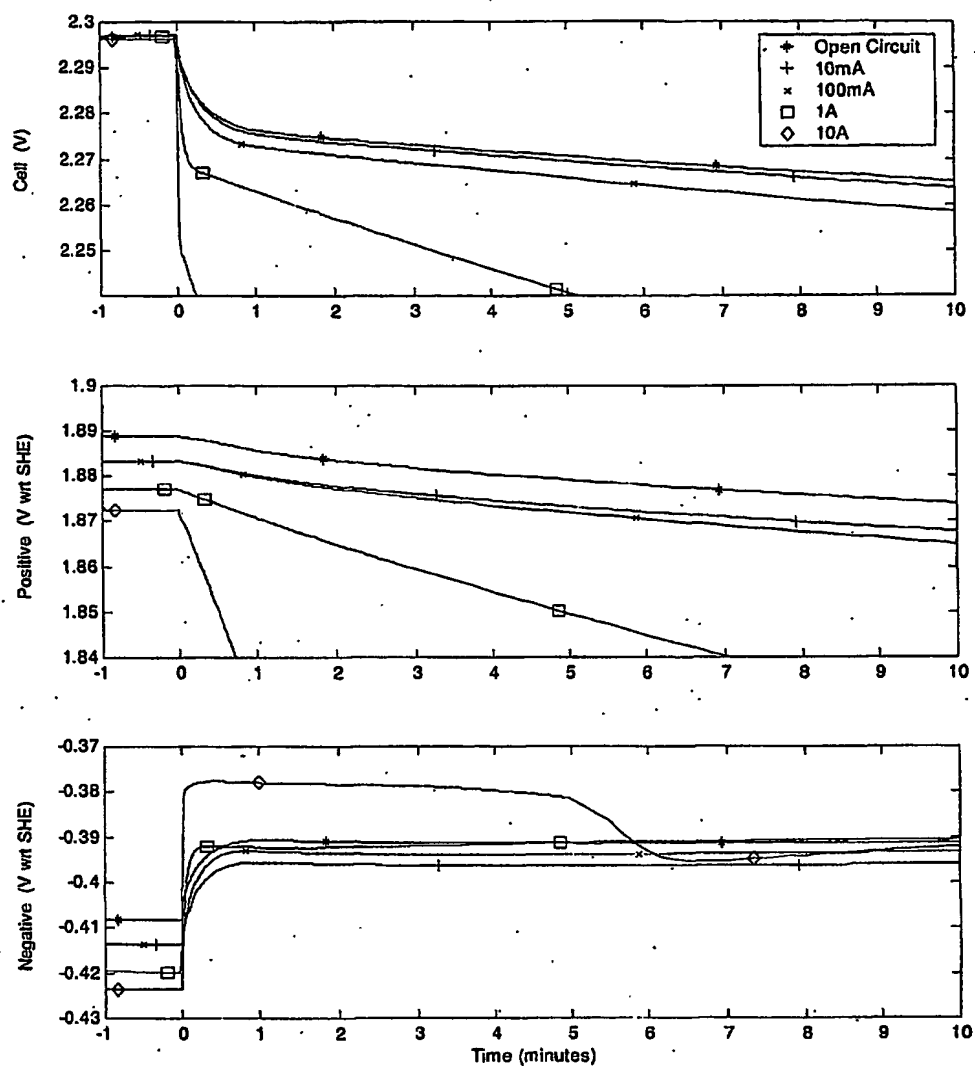


FIGURE 1



**FIGURE 2**





**FIGURE 3**

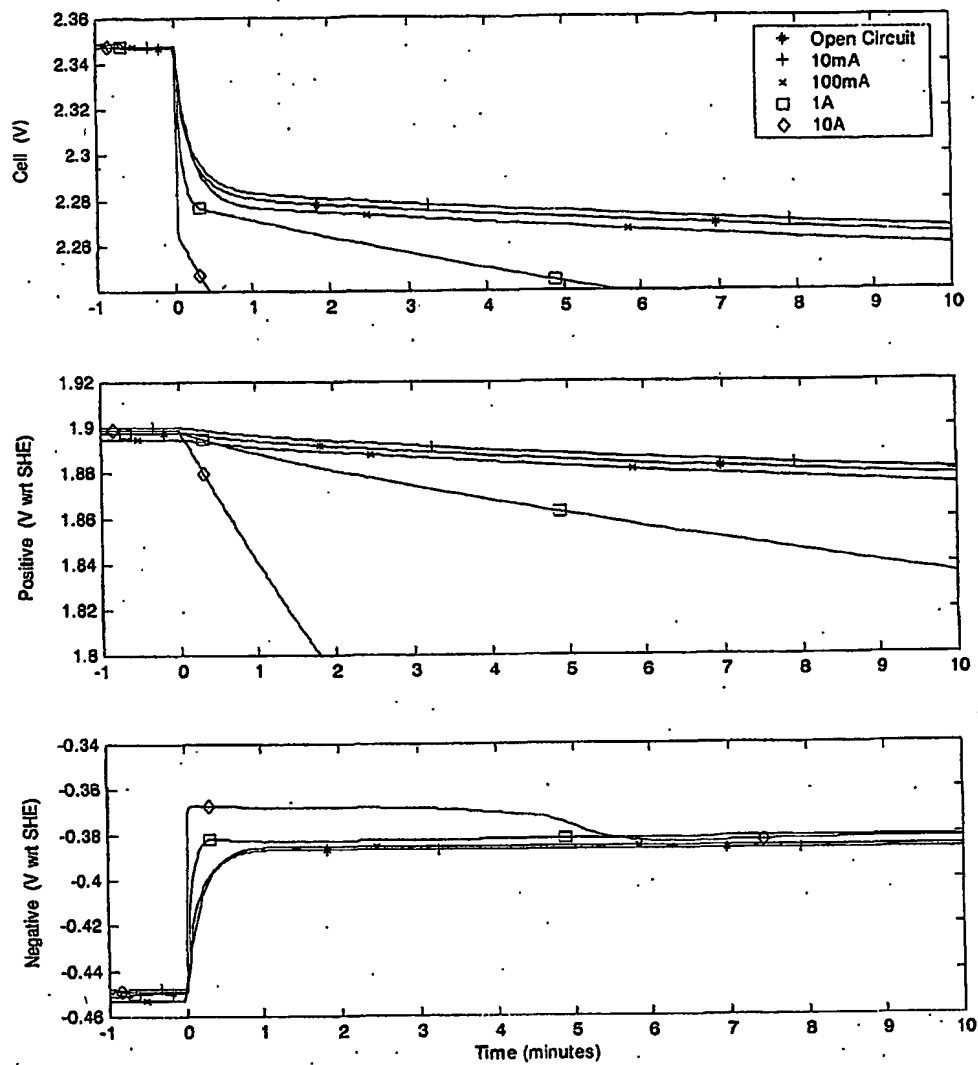


**FIGURE 4**

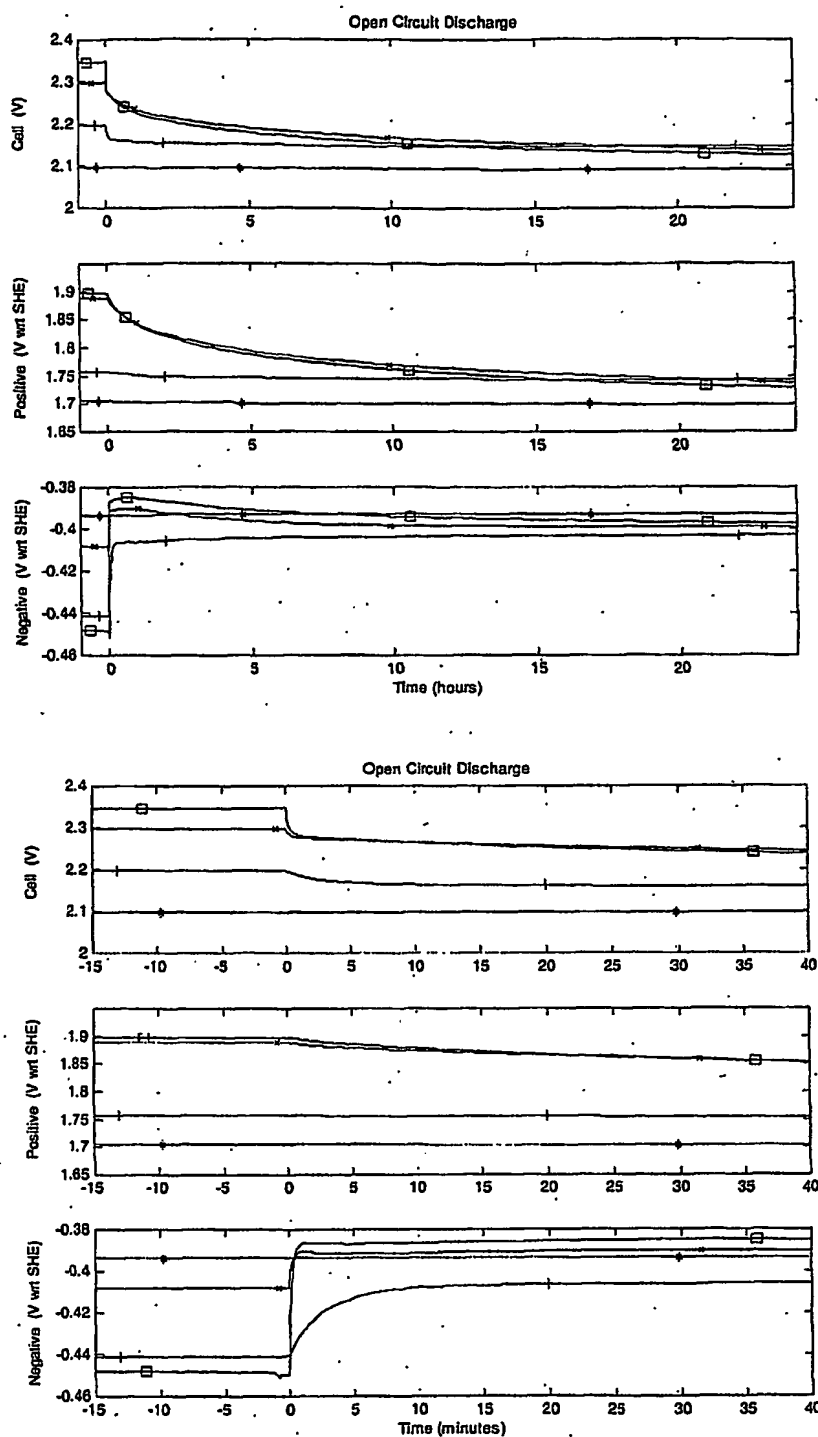
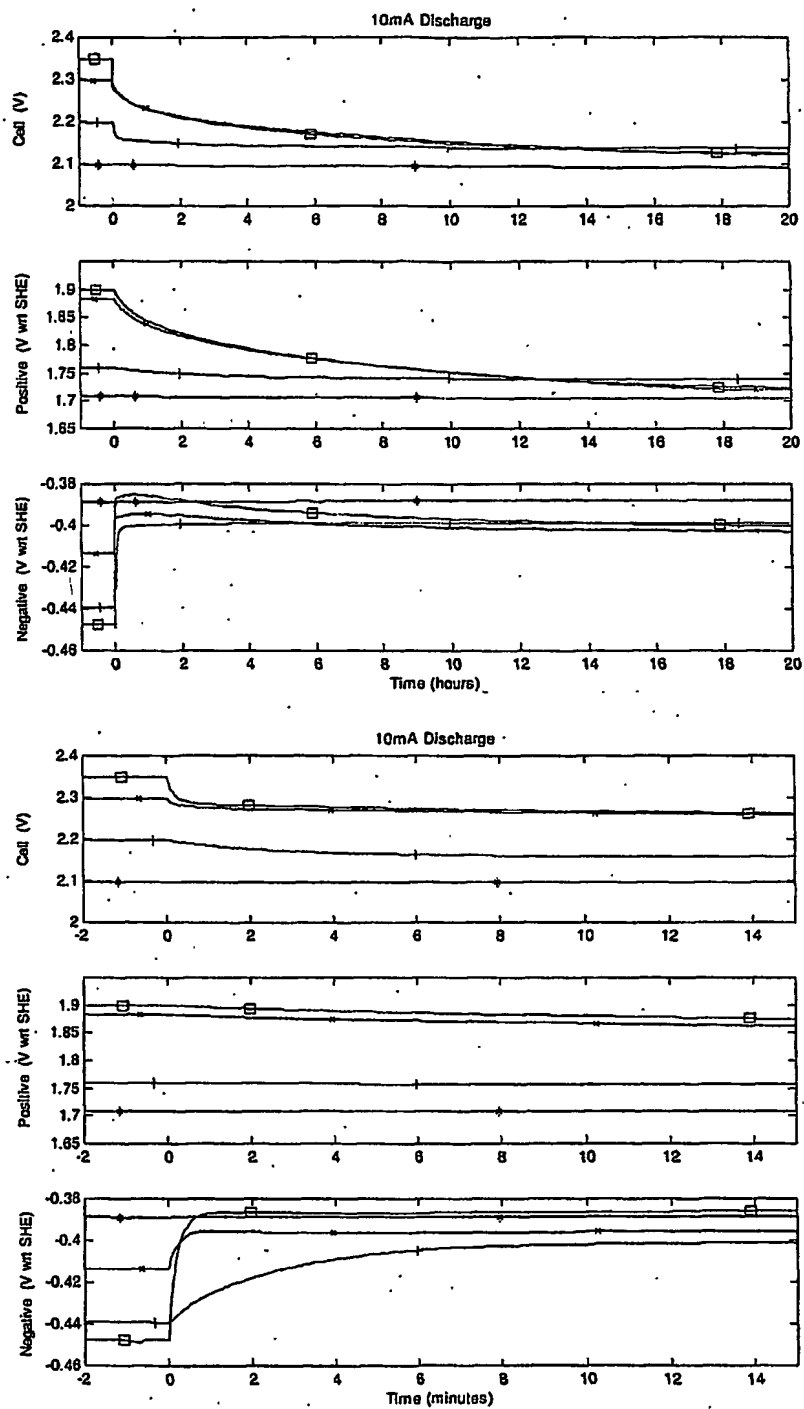


FIGURE 5



**FIGURE 6**

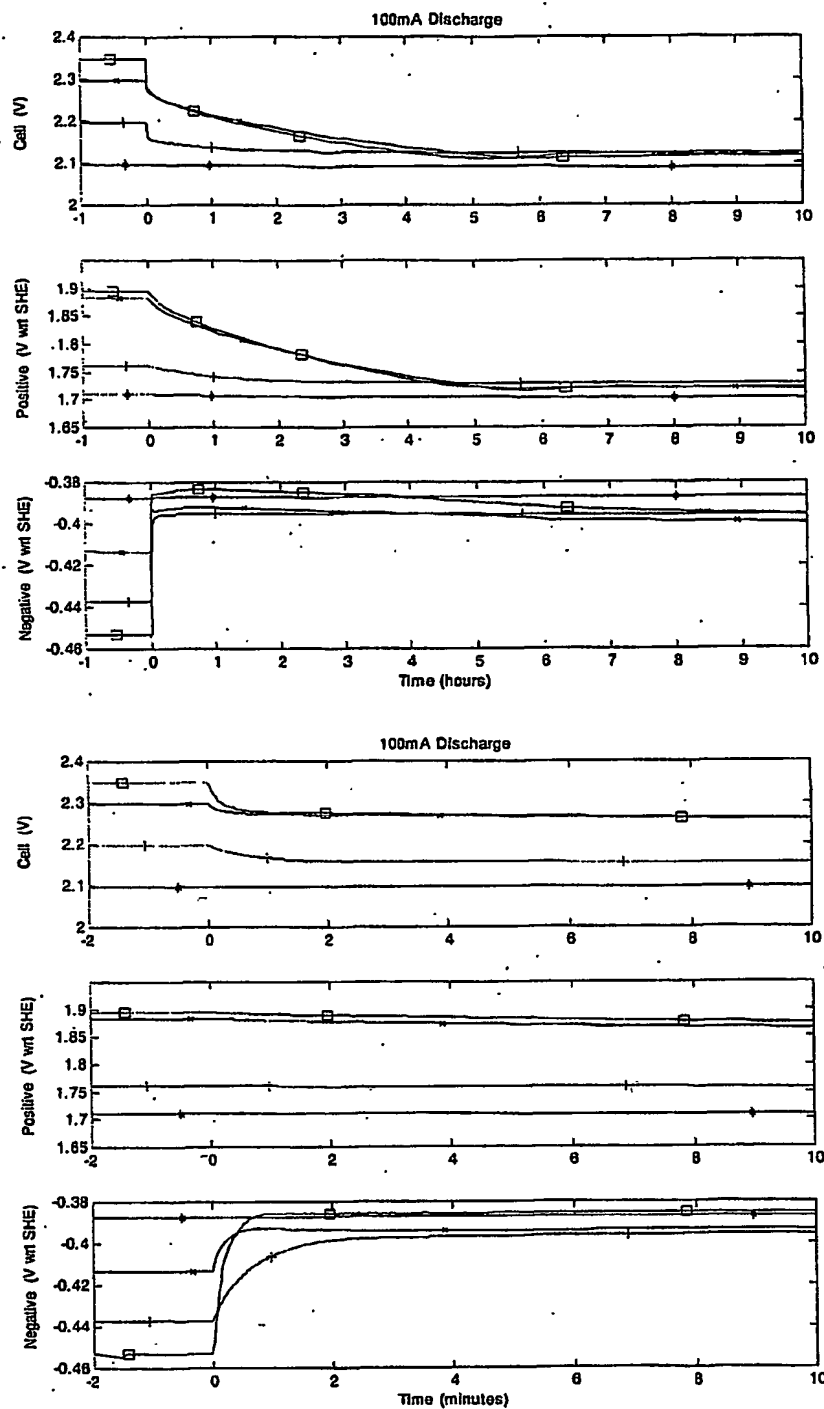
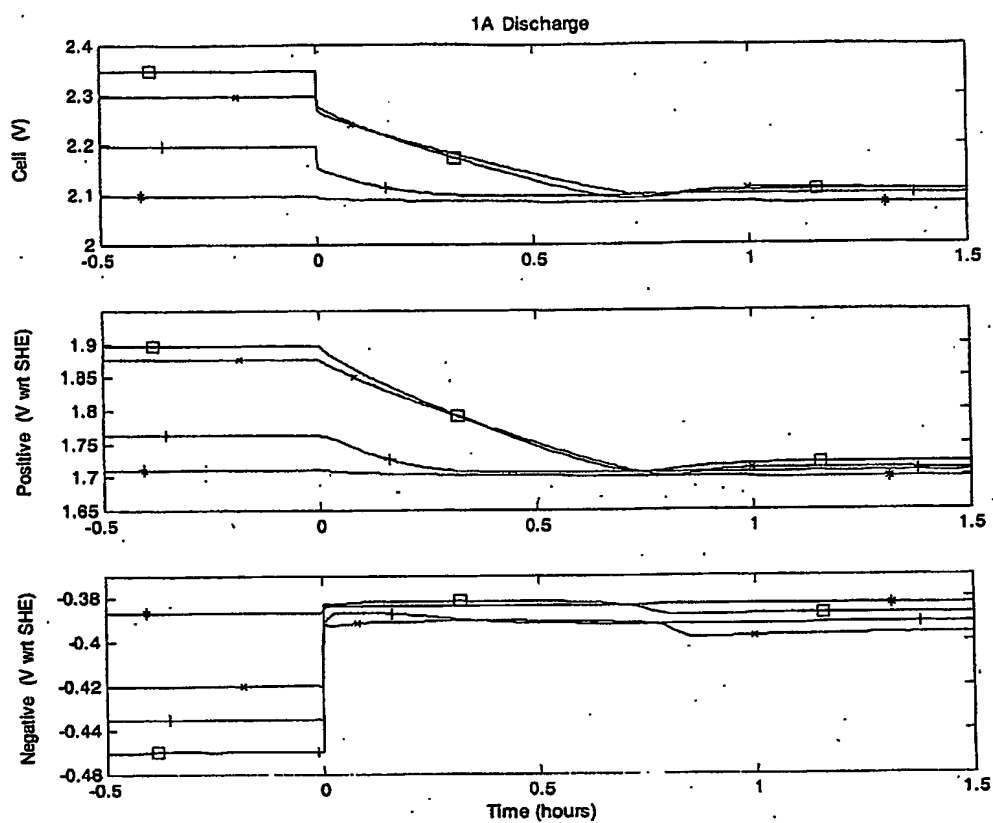
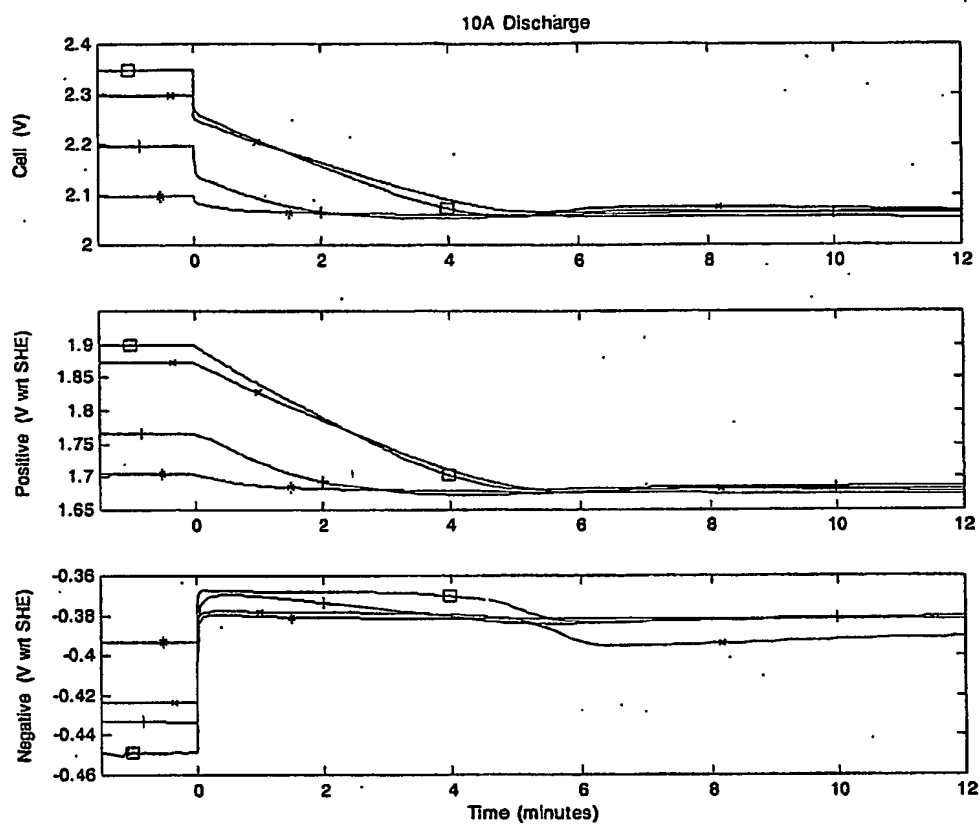


FIGURE 7



**FIGURE 8**



**FIGURE 9**

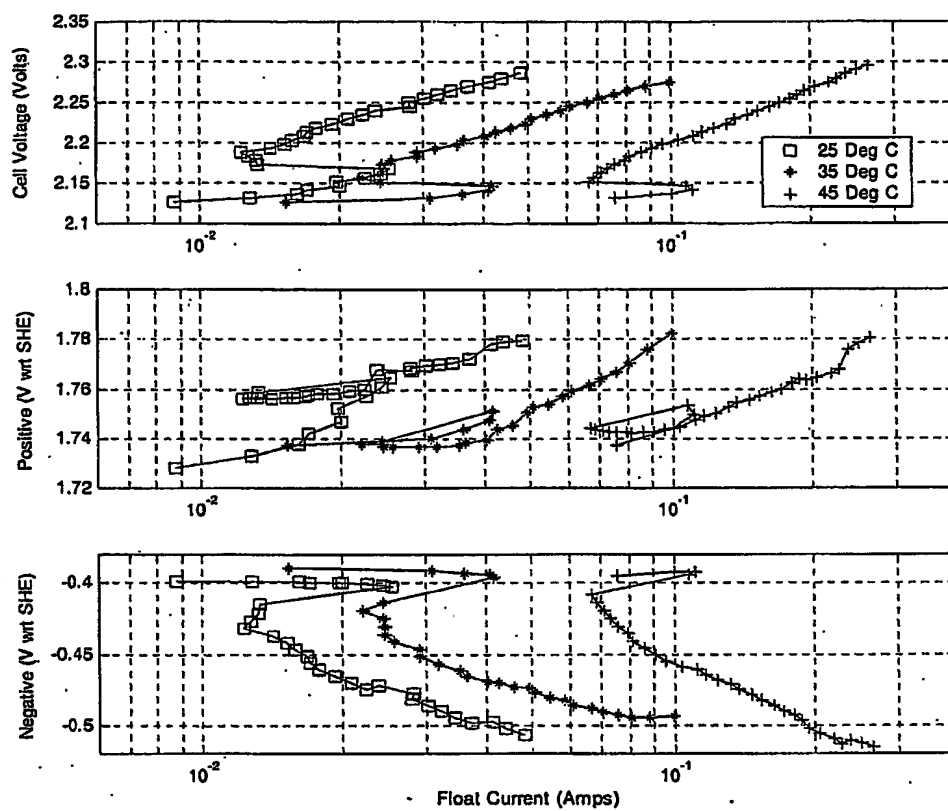


**FIGURE 10**



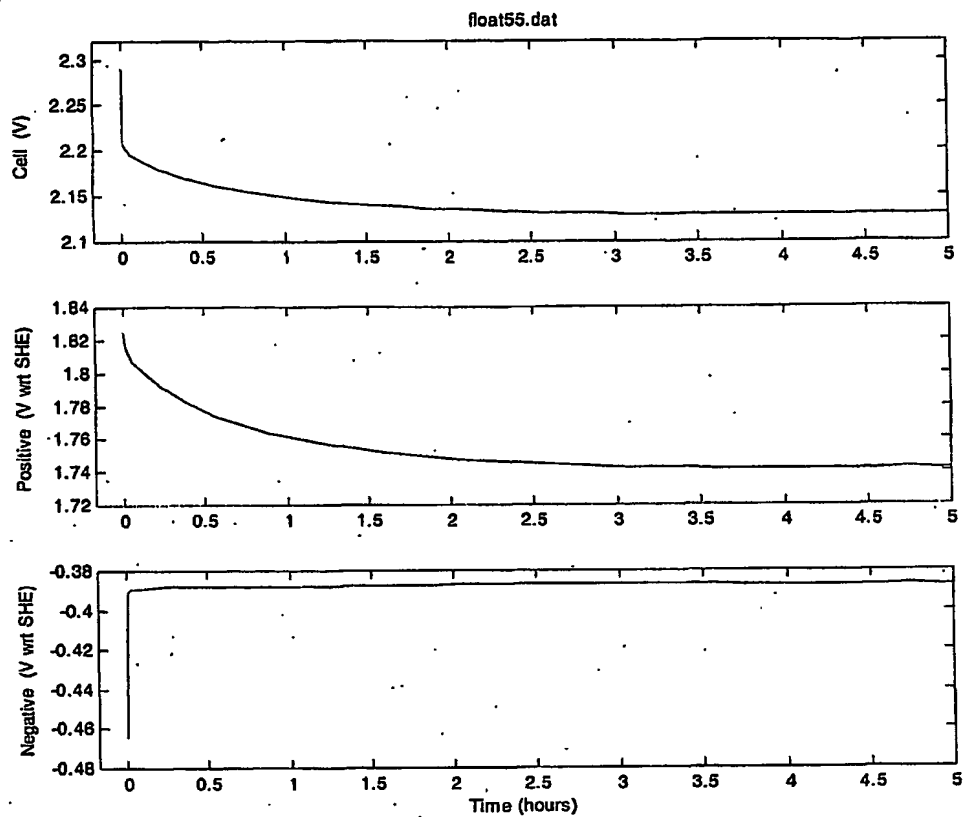


**FIGURE 11**

**This Page is Inserted by IFW Indexing and Scanning  
Operations and is not part of the Official Record**

**BEST AVAILABLE IMAGES**

Defective images within this document are accurate representations of the original documents submitted by the applicant.

Defects in the images include but are not limited to the items checked:

☐ BLACK BORDERS

☒ IMAGE CUT OFF AT TOP, BOTTOM OR SIDES

☒ FADED TEXT OR DRAWING

☒ BLURRED OR ILLEGIBLE TEXT OR DRAWING

☒ SKEWED/SLANTED IMAGES

☐ COLOR OR BLACK AND WHITE PHOTOGRAPHS

☒ GRAY SCALE DOCUMENTS

☒ LINES OR MARKS ON ORIGINAL DOCUMENT

☐ REFERENCE(S) OR EXHIBIT(S) SUBMITTED ARE POOR QUALITY

☐ OTHER: \_\_\_\_\_

**IMAGES ARE BEST AVAILABLE COPY.**

**As rescanning these documents will not correct the image problems checked, please do not report these problems to the IFW Image Problem Mailbox.**